 doi:10.20944/preprints202002.0394.v1

Suggestion of a framework of similarity laws for geometric distorted structures subjected to impact loading

Shuai Wang [a,b], Fei Xu [a,b,*], Xiaoyu Zhang [a,b], Zhen Dai [a,b]

[a] School of Aeronautics, Northwestern Polytechnical University, Xi'an 710072, Shaanxi, People's Republic of China.

[b] Institute for Computational Mechanics and Its Applications, Northwestern Polytechnical University, Xi'an 710072, Shaanxi, People's Republic of China.

[*]E-mail address: xufei@nwpu.edu.cn

ABSTRACT: A framework of similarity laws, termed oriented-density-length-velocity (ODLV) framework, is suggested for the geometric distorted structures subjected to impact loading. The distinct feature of this framework is that the newly proposed oriented dimensions, dimensionless numbers and scaling factors for physical quantity are explicitly expressed by the characteristic lengths of three spatial directions, which overcome the inherent defects that traditional scalar dimensional analysis could not express the effects of structural geometric characteristics and spatial directions for similarity. The non-scalabilities of geometrical distortion as well as other distortions such as different materials and gravity could be compensated by the reasonable correction for the impact velocity, the geometrical thickness and the density, when the proposed dimensionless number of equivalent stress is used between scaled model and prototype. Three analytical models of beam, plate and shell subjected to impact mass or impulsive velocity are verified by equation analysis. And a numerical model of circular plate subjected to dynamic pressure pulse is verified in more detail, form the

Preprints (www.preprints.org) | NOT PEER-REVIEWED | Posted: 26 February 2020 doi:10.20944/preprints202002.0394.v1

view of point of space deformation, deformation history and the components of displacement, strain and stress. The results show that the proposed dimensionless numbers have attractively perfect ability to express the dimensionless response equations of displacement, angle, time, strain and strain rate. When the proposed dimensionless numbers are used to regularize impact models, the structural responses of the geometrically distorted scaled models can behave the completely identical behaviors with those of the prototype on space and time —not only for the direction-independent equivalent stress, strain and strain rate but also for the direction-dependent displacement, stress and strain components.

Keywords: Dimensionless number; Similarity; Scaling; Geometric distortion; Structural impact.

1. Introduction

It is well known that the similarity laws for structures subjected to impact loading were systematically summarized by Jones (1989). In this work, twenty-two dimensionless numbers, based on the classical mass-length-time (MLT) dimensional analysis, were proposed, and the basic geometric scaling factor $\beta_{\bar{L}}$ was used to relate the physical quantities from scaled model to full-size prototype. The factor $\beta_{\bar{L}}$ was defined as $\beta_{\bar{L}} = \bar{L}_m/\bar{L}_p$, where β was scaling factor; $\bar{L}$ was the characteristic lengths of structure; the subscripts m and p represented the scaled model and the prototype, respectively. However, it must be used with great care because the scaling factors of MLT would become invalid when the material strain-rate-sensitivity, the gravity and

Preprints (www.preprints.org) | NOT PEER-REVIEWED | Posted: 26 February 2020 doi:10.20944/preprints202002.0394.v1

Nomenclature			
		$\alpha,\ \dot{\alpha},\ \ddot{\alpha}$	angle, angular velocity and angular acceleration, respectively
		α_f	final rotation angle
A	acceleration	β	scaling factor
B	width	γ	shear strain
c	dimensional constant	δ	displacement
D_n	Johnson's damage number	$\varepsilon,\ \dot{\varepsilon}$	strain and strain rate, respectively
E	energy	ε_f	permanent membrane strain
E'	elastic modulus	$\varepsilon_{eq},\ \dot{\varepsilon}_{eq}$	equivalent strain and strain rate, respectively
$F,\ F'$	force and inertia force, respectively	$\dot{\varepsilon}_{ave}$	average strain rate
g	gravity acceleration	ζ	$\zeta = B/L$
G	impact mass	η	distortion degree of thickness (β_H/β_R)
H	thickness	$\theta,\ \bar{\theta}$	angle and characteristic angle for cylindrical coordinates (r,θ,z), respectively
I	impulse	κ	mass ratio of impact mass to structure mass
$i,\ j$	$i,j = 1,2,3\ (or\ x,y,z)$	λ	$\lambda = (\mu V_0^2 L^2)/[(\sigma_0 H^2/4)H]$
k	$k = 3\ (or\ z)$	$\mu,\ \mu'$	mass per unit length and per unit surface area, respectively
$l,\ L,\ \bar{L},\ \bar{L}'$	length, half length, characteristic length and characteristic length of other-direction, respectively	ξ_0	$\xi_0 = \zeta\{[3+\zeta^2]^{1/2} - \zeta\}$
$m,\ M,\ \Delta M$	mass, structural mass and additional mass, respectively	π	circumference ratio
n	positive real number	Π	dimensionless number
N_0	full-plastic membrane force of rectangular section beam ($\sigma_d BH$)	ρ	density
N_0'	fully plastic membrane force for the shell cross-section ($\sigma_d H$)	σ	stress
P	impulse pressure	$\sigma_0,\ \sigma_d$	static and dynamic flow stress, respectively
$R,\ \bar{R}$	radius and characteristic radius, respectively	σ_{eq}	equivalent stress
R_n	Zhao's response numbers (Eq. (3))	τ	shear stress
S	section area	χ	a general direction
t	time	ω	dimensionless moment resistance at supports, ω=0 and 1 for simply and fully clamped supports.
T_f	final response time	Ψ	bending moment
u	displacement of neutral plane elements of plate on the x-axis	Ψ_0	fully plastic bending moment of rectangular section beam ($BH^2/4$)

Preprints (www.preprints.org) | NOT PEER-REVIEWED | Posted: 26 February 2020 doi:10.20944/preprints202002.0394.v1

v	displacement of neutral plane elements of plate on the y-axis	Ψ'_0	unit width plastic bending moment
V, V_0	velocity and initial impact velocity, respectively	Ω	$GV_0^2/(4\sigma_d H^3)$
w	displacement of neutral plane elements of plate on the z-axis	x, y, z	cartesian coordinate system (x, y, z)
W_f	maximum permanent transverse displacement (or radial displacement for shell)	r, θ, z	cylindrical coordinate system (r, θ, z)
Z	distance to the neutral plane of plates	r, α_a, α_b	spherical coordinates system (r, α_a, α_b)
$\mathbb{A}$	dimension of angle	$()_m$	scaled model
$\mathbb{L}$	dimension of length	$()_p$	prototype
$\mathbb{M}$	dimension of mass	$()^{mod}$	modification for physical quantity
$\mathbb{R}$	dimension of radius	$()^{cor}$	correction for physical quantity
$\mathbb{T}$	dimension of time	$\dim(X)$	dimension of physical quantity X

the fracture were taken into account (Jones, 1989; Lu and Yu, 2003). Many works had demonstrated the potential influence of these non-scalability for structural impact (Booth et al., 1983; Jones, 1989; Me-Bar, 1997; Jiang, et al., 2006a; Jiang, et al., 2006b; Li, et al., 2008; Fu, et al., 2018). A classic example was the work of Booth et al., which reported 13 drop tests on geometrically similar one-quarter-scale to full-scale structures for strain-rate-sensitive materials (Booth et al., 1983). The significant departures from similitude for the testing results revealed the nonnegligible influence of material strain-rate-sensitivity for similarity. In addition, since the geometric scaling factor β_L was used to equally scale the characteristic lengths of prototype configuration in different direction, the MLT system did not allow for the use of the scaled model with distorted geometric configuration.

It is vital that the non-scaling cases were more widespread than the perfect scaling ones due to the experimental difficulties in manufacturing scaled models where materials, geometry size and so on were often limited. Drazetic, et al. (1994) presented

Preprints (www.preprints.org) | NOT PEER-REVIEWED | Posted: 26 February 2020 doi:10.20944/preprints202002.0394.v1

a non-direct scaling technique, through reasonably correcting the impact velocity of scaled model, to address the distortion case that the mass, impact velocity, geometrical thickness and materials of scaled model did not satisfy the scaling of MLT. By improving this technique, Oshiro and Alves (2004) proposed the initial impact velocity V_0 - dynamic flow stress σ_d - impact mass G (VSG) dimensional analysis to address the material distortion of strain-rate-sensitivity. In the VSG system, the dimensionless numbers were expressed as follows:

$$\frac{A^3G}{V_0^4\sigma_d}, \frac{t^3\sigma_d V_0}{G}, \frac{\delta^3\sigma_d}{GV_0^2}, \dot{\varepsilon}\left(\frac{G}{\sigma_d V_0}\right)^{1/3}, \frac{\sigma}{\sigma_d}, \tag{1}$$

where A, t, δ, $\dot{\varepsilon}$ and σ were acceleration, time, displacement, strain rate (for strain ε) and stress, respectively. Based on this system, one more basic scaling factor β_V (V was velocity) was used to scale the behaviors of prototype by reasonably correcting the impact velocity and impact mass of scaled model (Oshiro and Alves, 2004; 2007; 2009; Alves and Oshiro, 2006a; 2006b). The material distortion for the difference of density, yield stress and strain-rate-sensitivity between scaled model and prototype can also be compensated by increasing one more number $\frac{M}{G}$ and one more basic factor β_ρ into the VSG system, where M and ρ were structure mass and density, respectively (Mazzariol, et al., 2016). The solutions of material distortion, further including material strain hardening effects, were verified by a group of transport equations of the continuum mechanics in the work of Sadeghi, et al. (2019a; 2019b). In addition, a new technique —adding extra mass to correct the density of structure, was proposed to compensate the non-scalability of gravity and material strain-rate-sensitivity (Jiang et al., 2016; Wei and Hu, 2019). The above studies formed a new similarity laws of

Preprints (www.preprints.org) | NOT PEER-REVIEWED | Posted: 26 February 2020 doi:10.20944/preprints202002.0394.v1

structural impact which using three basic scaling factors $\beta_{\bar{L}}$, β_V and β_ρ to relate physical quantities from scaled model to prototype. The main scaling factors of VSG system were listed in Table 1.

Table 1 Main scaling factors in VSG.

Variable	Scaling factor	Variable	Scaling factor
Length, $\bar{L}$	$\beta_{\bar{L}} = \bar{L}_m/\bar{L}_p$	Displacement, δ	$\beta_\delta = \beta_{\bar{L}}$
Density, ρ	$\beta_\rho = \rho_m/\rho_p$	Stress, σ	$\beta_\sigma = \beta_\rho\beta_V^2$
Velocity, V	$\beta_V = V_m/V_p$	Strain, ε	$\beta_\varepsilon = 1$
Mass, m	$\beta_m = \beta_\rho\beta_{\bar{L}}^3$	Strain rate, $\dot{\varepsilon}$	$\beta_{\dot{\varepsilon}} = \beta_V/\beta_{\bar{L}}$
Time, t	$\beta_t = \beta_{\bar{L}}/\beta_V$	Acceleration, A	$\beta_A = \beta_V^2/\beta_{\bar{L}}$

Although the addressing ability for distortion problems was effectively extended, for the scaled model with geometric distorted configuration, the VSG system was still invalid. Based on the VSG scaling factors, Oshiro and Alves (2012) presented an indirect method for the geometric distortion structures, where the iterative scaling testing were used to determine the unknown parameter of distorted scaling factors. However, because of its obvious defects that based on the experience of researchers and the numerous tests, the indirect method cannot be practical for a wide range of applications. In addition, since different unknown parameters need to be tested for different physical quantities, the indirect method was difficult to use for the comprehensive relations from scaled model to prototype.

In order to extend the application of dimensionless numbers for explanation of physical meaning, expression of response equations and scaling analysis, Wang, Xu and

Preprints (www.preprints.org) | NOT PEER-REVIEWED | Posted: 26 February 2020 doi:10.20944/preprints202002.0394.v1

Dai (2019) proposed the density-length-velocity (DLV) dimensional analysis, instead of the VSG system, to express the similarity laws of structural impact. In the DLV system, fifteen dimensionless numbers were expressed as follows:

$$\frac{\rho V^2}{\sigma_d},\frac{\rho \bar{L}^2 V^2}{F},\frac{\rho \bar{L}^3 V^2}{\Psi},\frac{tV}{\bar{L}},\frac{\dot{\varepsilon}\bar{L}}{V},\frac{A\bar{L}}{V^2},\frac{\dot{\alpha}\bar{L}}{V},\frac{\ddot{\alpha}\bar{L}^2}{V^2},\\ \frac{E}{\rho \bar{L}^3 V^2},\frac{I}{\rho \bar{L}^3 V},\frac{m}{\rho \bar{L}^3},\frac{\bar{L}'}{\bar{L}},\frac{\delta}{\bar{L}},\varepsilon,\alpha, \tag{2}$$

where F, Ψ, α, $\dot{\alpha}$, $\ddot{\alpha}$, E, I and $\bar{L}'$ were force, bending moment, angle, angular velocity, angular acceleration, energy, impulse and characteristic length of other-direction (e.g., thickness H and width B), respectively. Meanwhile the same scaling factors as VSG are used to address the distortion of different materials by the correction for the impact velocity and the density (or structure and impact mass) of scaled model. In addition, some important improvements were that the Johnson's damage number $D_n = \frac{\rho V_0^2}{\sigma_0}$ (Johnson, 1972; Zhao, 1998a) was expressed by the number $\frac{\rho V^2}{\sigma_d}$, where σ_0 was static flow stress; the Zhao's response number $R_n = \frac{\rho V_0^2}{\sigma_0}\left(\frac{\bar{L}}{H}\right)$ was naturally expressed by the number $\frac{\rho \bar{L}^2 V^2}{N_0} = \left[\frac{\rho V_0^2}{\sigma_d}\left(\frac{\bar{L}}{H}\right)\right]\frac{\bar{L}}{B}$ for the full-plastic membrane force of rectangular section beam $N_0 = \sigma_d BH$; and the Zhao's response number $R_n = \frac{\rho V_0^2}{\sigma_0}\left(\frac{\bar{L}}{H}\right)^2$ was naturally expressed by the number $\frac{\rho \bar{L}^3 V^2}{\Psi_0} = 4\left[\frac{\rho V_0^2}{\sigma_d}\left(\frac{\bar{L}}{H}\right)^2\right]\frac{\bar{L}}{B}$ for the full-plastic moment of rectangular section beam $\Psi_0 = \sigma_d BH^2/4$. The Zhao's response numbers R_n, usually used to measure the response of impacted structures (Zhao, 1998b; 1999; Li and Jones, 2000; Shi and Gao, 2001; Hu, 2000; 2009), are defined as

$$R_n(n) = \frac{\rho V_0^2}{\sigma_0}\left(\frac{\bar{L}}{H}\right)^2, \frac{\rho V_0^2}{\sigma_0}\left(\frac{\bar{L}_a}{\bar{L}_b}\right)^n, \frac{\rho V_0^2}{E'}\left(\frac{\bar{L}_a}{\bar{L}_b}\right)^n, et\ al, \tag{3}$$

where E' and n are elastic modulus and positive real number, respectively; $\bar{L}_a$ and

Preprints (www.preprints.org) | NOT PEER-REVIEWED | Posted: 26 February 2020 doi:10.20944/preprints202002.0394.v1

$\bar{L}_b$ are two characteristic lengths of different directions. It is evident from the DLV numbers that characteristic lengths of different directions were clearly expressed in some numbers, which reflected the influence of different geometric characteristics for structural scaled behaviors. Nevertheless, the DLV system also had no ability to directly express the geometric distorted structures due to the use of single characteristic length $\bar{L}$ in most dimensionless numbers.

Recently, Mazzariol and Alves (2019a; b) presented a direct method for the geometric distorted structures. In the new method, the velocity-dynamic flow stress-structure mass (VSM) dimensional analysis, instead of the VSG system, was used to express dimensionless numbers as follows:

$$\frac{A^3M}{V^4\sigma_d},\frac{t^3\sigma_dV}{M},\frac{\delta^3\sigma_d}{MV^2},\frac{\dot{\varepsilon}^3M}{\sigma_dV},\frac{\sigma}{\sigma_d},\frac{\Psi'^3_0}{V^4\sigma_dM^2},\frac{\rho V^2}{\sigma_d},\frac{M}{G}, \tag{4}$$

where Ψ'_0 was unit width plastic bending moment. In the meantime, six basic scaling factors β_χ, β_{σ_d}, β_M, β_H, β_{V_χ} and β_ρ formed the scaling factors of VSM, listed in Table 2, where χ was a general direction; $\beta_M=\beta_\rho\beta_L\beta_B\beta_H$ for cartesian coordinates (L, H, B) and $\beta_M=\beta_\rho\beta_R^2\beta_H$ for cylindrical coordinates (R, H); R was radius.

Table 2 Main scaling factors in VSM.

Variable	Scaling factor	Variable	Scaling factor
Dimension, χ	β_χ	Displacement, δ_χ	$\beta_{\delta_\chi}=\beta_\chi$
Density, ρ	$\beta_\rho=\rho_m/\rho_p$	Stress, σ	$\beta_\sigma=\beta_{\sigma_d}$
Velocity, V	$\beta_V=\left(\beta_H^3\beta_{\sigma_d}/\beta_M\right)^{1/2}$	Strain, ε	$\beta_\varepsilon=1$

Preprints (www.preprints.org) | NOT PEER-REVIEWED | Posted: 26 February 2020 doi:10.20944/preprints202002.0394.v1

Impact mass, G	$\beta_G = \beta_M$	Strain rate, $\dot{\varepsilon}$	$\beta_{\dot{\varepsilon}} = \beta_H/\beta_{V_\chi}$
Time, t	$\beta_t = \beta_\chi/\beta_{V_\chi}$	Force, F	$\beta_F = \beta_H^2\beta_{\sigma_d}$
Acceleration, A	$\beta_A = \beta_H^2\beta_{\sigma_d}/\beta_M$	Energy, E	$\beta_E = \beta_H^3\beta_{\sigma_d}$

Compared with the indirect method of Oshiro and Alves (2012), the scaling factors for geometric thickness distortion are explicitly and directly expressed by VSM. Nevertheless, three main defects were easily discovered in VSM. (1) Some scaling factors would be unreasonable. For example, the displacement factor $\beta_{\delta_\chi} = \beta_\chi$ would include the case of thickness distortion (i.e., $\beta_\delta = \beta_H \neq \beta_L$) but the strain factor $\beta_\varepsilon = 1$ does not. The self-contradictory phenomenon indicates the factor $\beta_\varepsilon = 1$ is unreasonable for thickness distortion case. (2) The number $\frac{\rho V^2}{\sigma_d}$ cannot be applied to the geometric distortion. It is evident from the form $\frac{\rho V^2}{\sigma_d}$ that the velocity was independent of the geometric thickness, which was inconsistent with the factor $\beta_V = \left(\beta_H^3\beta_{\sigma_d}/\beta_M\right)^{1/2}$ of Table 2. (3) Components of displacement, stress, strain, strain rate and velocity are not explicitly expressed in the VSM system. These difficulties formed the basic motivation for further development of new dimensional analysis framework in this paper.

In what follows, Sect. 2 introduced our newly proposed ODLV similarity law framework. Section 3 investigated three analytical models of beam, plate and shell subjected to impact mass or impulsive velocity. Section 4 investigated a numerical model of circular plate subjected to dynamic pressure pulse. Sect. 5 summarized this work.

Preprints (www.preprints.org) | NOT PEER-REVIEWED | Posted: 26 February 2020 doi:10.20944/preprints202002.0394.v1

2. The ODLV similarity laws

2.1. Assumptions

In order to re-derive the similarity laws of impact problems, we assume that the mechanical mechanism for geometric distorted impacted structures is the same as that of an initial flat thin-plate subjected to transverse impact loading. The thin-plate has the arbitrary shape and boundary conditions and is subjected to transverse impact loading, as shown in Fig. 1. The impact model of thin-plate is built in the cartesian coordinate system (x, y, z). The subscripts x, y and z represent the x-axis direction, the y-axis direction and the z-axis direction, respectively; the subscripts xy, xz and yz represent the x-y plane direction, the x-z plane direction and the y-z plane direction, respectively.

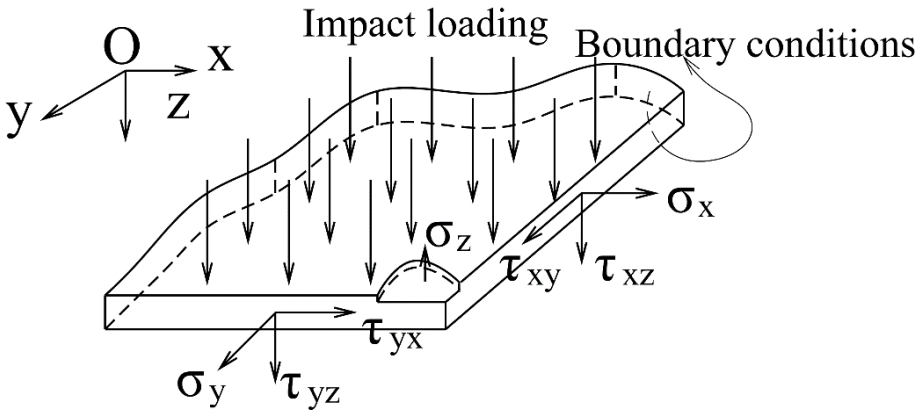

Fig. 1 A thin-plate structure subjected to transverse impact.

The following simplifications are assumed: (1) The structure is assumed to be made of the isotropic and rigid-plastic materials including strain-hardening and strain-rate-sensitivity. (2) Under the thin-plate assumption, the transverse shear deformation and the change of deflection in the thickness direction are not taken into account, i.e. $\gamma_{xz} = \gamma_{yz} = \varepsilon_z = 0$ and $\tau_{xz} = \tau_{yz} = \sigma_z = 0$, where γ and τ are shear strain and

Preprints (www.preprints.org) | NOT PEER-REVIEWED | Posted: 26 February 2020 doi:10.20944/preprints202002.0394.v1

shear stress, respectively. (3) Strain components are expressed as $\varepsilon_x = \left(\frac{\partial u}{\partial x}\right) + \frac{1}{2}\left(\frac{\partial w}{\partial x}\right)^2 - \left(Z\frac{\partial^2 w}{\partial x^2}\right)$, $\varepsilon_y = \left(\frac{\partial v}{\partial y}\right) + \frac{1}{2}\left(\frac{\partial w}{\partial y}\right)^2 - \left(Z\frac{\partial^2 w}{\partial y^2}\right)$, $\gamma_{xy} = \left(\frac{\partial u}{\partial y} + \frac{\partial v}{\partial x}\right) + \left(\frac{\partial w}{\partial x}\frac{\partial w}{\partial y}\right) - \left(2Z\frac{\partial^2 w}{\partial x \partial y}\right)$, $\gamma_{xz} = \left(-\frac{\partial w}{\partial x}\right) + \left(\frac{\partial w}{\partial x}\right) = 0$, $\gamma_{yz} = \left(-\frac{\partial w}{\partial y}\right) + \left(\frac{\partial w}{\partial y}\right) = 0$ and $\varepsilon_z = \left(\frac{\partial w}{\partial z}\right) = 0$ (Reddy., 2007), where u, v and w are the displacement of neutral plane elements on the x-axis, the y-axis and the z-axis, respectively; Z is the distance to the neutral plane. The first two terms for ε_x, ε_y and γ_{xy} represent the strain from neutral plane and the last term represents the bending strain from deflection. (4) The displacement components of thin-plate problem are expressed as $\delta_x = u - \left(Z\frac{\partial w}{\partial x}\right)$, $\delta_y = v - \left(Z\frac{\partial w}{\partial y}\right)$ and $\delta_z = w$ where the terms $\left(Z\frac{\partial w}{\partial x}\right)$ and $\left(Z\frac{\partial w}{\partial y}\right)$ represent two in-plane displacements from deflection (Reddy., 2007).

Although the above assumptions come from the thin-plate problem, the following derivation and analyses could be applied to more complex structures, such as the stiffened plates.

2.2. Dimensionless numbers

Different from previous authors, three notations $\mathbb{L}_x$, $\mathbb{L}_y$ and $\mathbb{L}_z$ are used to present three oriented dimensions of length in the spatial directions x, y and z, respectively (Huntley., 1952; Chien., 1993). The oriented dimensional analysis extends three basic dimensions, i.e. mass dimension $\mathbb{M}$, scalar length dimension $\mathbb{L}$ and time dimension $\mathbb{T}$, to five basic dimensions, i.e. mass dimension $\mathbb{M}$, oriented length dimensions $\mathbb{L}_x$, $\mathbb{L}_y$, $\mathbb{L}_z$ and time dimension $\mathbb{T}$. Therefore, it enhances the power of dimensional analysis for expressing different spatial directions.

Preprints (www.preprints.org) | NOT PEER-REVIEWED | Posted: 26 February 2020 doi:10.20944/preprints202002.0394.v1

When structures are subjected to transverse impact loading, thirty basic physical quantities and their corresponding dimensions, proposed by simple physical definition, are listed in Table 3. The way to obtain these oriented dimensions is to reasonably analyze the definition of physical quantities. For example, the dimension $\mathbb{L}_x\mathbb{L}_y^{-1}\mathbb{L}_z^{-1}\mathbb{M}\mathbb{T}^{-2}$ of σ_x can be determined through the oriented dimension analysis $dim\left(F_x'/S_{yz}\right) = dim(F_x')/dim\left(S_{yz}\right) = (\mathbb{M}\mathbb{L}_x\mathbb{T}^{-2})\left(\mathbb{L}_y\mathbb{L}_z\right)^{-1}$ for the elementary definition $\sigma_x = F_x'/S_{yz}$, where 'dim (X)' represents the dimension of physical quantity X, F' and S are inertia force and section area, respectively; the dimension $\mathbb{L}_z^{-1}\mathbb{M}\mathbb{T}^{-2}$ of τ_{xy} can be determined through the oriented dimension analysis $dim\left(F_y'/S_{yz}\right) = dim\left(F_y'\right)/dim\left(S_{yz}\right) = \left(\mathbb{M}\mathbb{L}_y\mathbb{T}^{-2}\right)\left(\mathbb{L}_y\mathbb{L}_z\right)^{-1}$ for the elementary definition $\tau_{xy} = F_y'/S_{yz}$; the dimension $\mathbb{L}_x^{-2}\mathbb{L}_z^2$ of ε_x can be determined through the oriented dimension analysis $dim\left(\frac{\partial u}{\partial x}\right) = dim\left(\frac{1}{2}\left(\frac{\partial w}{\partial x}\right)^2\right) = dim\left(Z\frac{\partial^2 w}{\partial x^2}\right) = \mathbb{L}_x^{-2}\mathbb{L}_z^2$ for the definition $\varepsilon_x = \left(\frac{\partial u}{\partial x}\right) + \frac{1}{2}\left(\frac{\partial w}{\partial x}\right)^2 - \left(Z\frac{\partial^2 w}{\partial x^2}\right)$, which requires the dimension of u must be taken as $\mathbb{L}_x^{-1}\mathbb{L}_z^2$ according to the principle of dimensional homogeneity; the dimension 1 for ε_z can be determined through the oriented dimension analysis $dim\left(\frac{\partial w}{\partial z}\right) = 1$ for the definition $\varepsilon_z = \left(\frac{\partial w}{\partial z}\right)$; the dimension $\mathbb{L}_x^{-1}\mathbb{L}_z$ of γ_{xz} can be determined through the oriented analysis $dim\left(-\frac{\partial w}{\partial x}\right) = dim\left(\frac{\partial w}{\partial x}\right) = \mathbb{L}_x^{-1}\mathbb{L}_z$ for the definition $\gamma_{xz} = \left(-\frac{\partial w}{\partial x}\right) + \left(\frac{\partial w}{\partial x}\right)$; the dimension $\mathbb{L}_x^{-1}\mathbb{L}_z^2$ of δ_x can be determined through the oriented dimension analysis $dim(u) = dim\left(Z\frac{\partial w}{\partial x}\right) = \mathbb{L}_x^{-1}\mathbb{L}_z^2$ for the definition $\delta_x = u - \left(Z\frac{\partial w}{\partial x}\right)$.

Table 3 Oriented dimensions of main physical quantity.

Physical quantity	Dimension	Physical quantity	Dimension

Preprints (www.preprints.org) | NOT PEER-REVIEWED | Posted: 26 February 2020 doi:10.20944/preprints202002.0394.v1

Density ρ	$\mathbb{M}\mathbb{L}_x^{-1}\mathbb{L}_y^{-1}\mathbb{L}_z^{-1}$	Shear strain γ_{xz}	$\mathbb{L}_x^{-1}\mathbb{L}_z$
Length $\bar{L}_x$	$\mathbb{L}_x$	Shear strain γ_{yz}	$\mathbb{L}_y^{-1}\mathbb{L}_z$
Length $\bar{L}_y$	$\mathbb{L}_y$	Strain rate $\dot{\varepsilon}_x$	$\mathbb{L}_x^{-2}\mathbb{L}_z^2\mathbb{T}^{-1}$
Length $\bar{L}_z$	$\mathbb{L}_z$	Strain rate $\dot{\varepsilon}_y$	$\mathbb{L}_y^{-2}\mathbb{L}_z^2\mathbb{T}^{-1}$
Velocity V_z	$\mathbb{L}_z\mathbb{T}^{-1}$	Strain rate $\dot{\varepsilon}_z$	$\mathbb{T}^{-1}$
Normal stress σ_x	$\mathbb{L}_x\mathbb{L}_y^{-1}\mathbb{L}_z^{-1}\mathbb{M}\mathbb{T}^{-2}$	Strain rate $\dot{\gamma}_{xy}$	$\mathbb{L}_x^{-1}\mathbb{L}_y^{-1}\mathbb{L}_z^2\mathbb{T}^{-1}$
Normal stress σ_y	$\mathbb{L}_x^{-1}\mathbb{L}_y\mathbb{L}_z^{-1}\mathbb{M}\mathbb{T}^{-2}$	Strain rate $\dot{\gamma}_{xz}$	$\mathbb{L}_x^{-1}\mathbb{L}_z\mathbb{T}^{-1}$
Normal stress σ_z	$\mathbb{L}_x^{-1}\mathbb{L}_y^{-1}\mathbb{L}_z\mathbb{M}\mathbb{T}^{-2}$	Strain rate $\dot{\gamma}_{yz}$	$\mathbb{L}_y^{-1}\mathbb{L}_z\mathbb{T}^{-1}$
Shear stress τ_{xy}	$\mathbb{L}_z^{-1}\mathbb{M}\mathbb{T}^{-2}$	Time t	$\mathbb{T}$
Shear stress τ_{xz}	$\mathbb{L}_y^{-1}\mathbb{M}\mathbb{T}^{-2}$	Displacement δ_x	$\mathbb{L}_x^{-1}\mathbb{L}_z^2$
Shear stress τ_{yz}	$\mathbb{L}_x^{-1}\mathbb{M}\mathbb{T}^{-2}$	Displacement δ_y	$\mathbb{L}_y^{-1}\mathbb{L}_z^2$
Normal strain ε_x	$\mathbb{L}_x^{-2}\mathbb{L}_z^2$	Displacement δ_z	$\mathbb{L}_z$
Normal strain ε_y	$\mathbb{L}_y^{-2}\mathbb{L}_z^2$	Structure mass M	$\mathbb{M}$
Normal strain ε_z	1	Impact mass G	$\mathbb{M}$
Shear strain γ_{xy}	$\mathbb{L}_x^{-1}\mathbb{L}_y^{-1}\mathbb{L}_z^2$	Impulse pressure P_z	$\mathbb{L}_x^{-1}\mathbb{L}_y^{-1}\mathbb{L}_Z\mathbb{M}\mathbb{T}^{-2}$

Based on the previous DLV system, the density ρ, the characteristic lengths $\bar{L}_x$, $\bar{L}_y$, $\bar{L}_z$ and the velocity V_z are chosen as base to derive dimensionless numbers. When using the Buckingham Π theorem (Buckingham, 1914; 1915), thirty basic physical quantities of Table 3 can be reduced to twenty-five dimensionless numbers, as follows:

- six stress components

Preprints (www.preprints.org) | NOT PEER-REVIEWED | Posted: 26 February 2020 doi:10.20944/preprints202002.0394.v1

$$\Pi_{\sigma_x}=\left[\frac{\rho V_z^2}{\sigma_x}\left(\frac{\bar{L}_x}{\bar{L}_z}\right)^2\right],\Pi_{\sigma_y}=\left[\frac{\rho V_z^2}{\sigma_y}\left(\frac{\bar{L}_y}{\bar{L}_z}\right)^2\right],\Pi_{\sigma_z}=\left[\frac{\rho V_z^2}{\sigma_z}\right],$$
$$\Pi_{\tau_{xy}}=\left[\frac{\rho V_z^2}{\tau_{xy}}\left(\frac{\sqrt{\bar{L}_x\bar{L}_y}}{\bar{L}_z}\right)^2\right],\Pi_{\tau_{xz}}=\left[\frac{\rho V_z^2}{\tau_{xz}}\left(\frac{\bar{L}_x}{\bar{L}_z}\right)\right],\Pi_{\tau_{yz}}=\left[\frac{\rho V_z^2}{\tau_{yz}}\left(\frac{\bar{L}_y}{\bar{L}_z}\right)\right]; \quad (5a\text{-}f)$$

- six strain components

$$\Pi_{\varepsilon_x}=\left[\varepsilon_x\left(\frac{\bar{L}_x}{\bar{L}_z}\right)^2\right],\Pi_{\varepsilon_y}=\left[\varepsilon_y\left(\frac{\bar{L}_y}{\bar{L}_z}\right)^2\right],\Pi_{\varepsilon_z}=[\varepsilon_z],$$
$$\Pi_{\gamma_{xy}}=\left[\gamma_{xy}\left(\frac{\sqrt{\bar{L}_x\bar{L}_y}}{\bar{L}_z}\right)^2\right],\Pi_{\gamma_{xz}}=\left[\gamma_{xz}\left(\frac{\bar{L}_x}{\bar{L}_z}\right)\right],\Pi_{\gamma_{yz}}=\left[\gamma_{yz}\left(\frac{\bar{L}_y}{\bar{L}_z}\right)\right]; \quad (6a\text{-}f)$$

- six strain rate components

$$\Pi_{\dot{\varepsilon}_x}=\left[\frac{\dot{\varepsilon}_x\bar{L}_z}{V_z}\left(\frac{\bar{L}_x}{\bar{L}_z}\right)^2\right],\Pi_{\dot{\varepsilon}_y}=\left[\frac{\dot{\varepsilon}_y\bar{L}_z}{V_z}\left(\frac{\bar{L}_y}{\bar{L}_z}\right)^2\right],\Pi_{\dot{\varepsilon}_z}=\left[\frac{\dot{\varepsilon}_z\bar{L}_z}{V_z}\right],$$
$$\Pi_{\dot{\gamma}_{xy}}=\left[\frac{\dot{\gamma}_{xy}\bar{L}_z}{V_z}\left(\frac{\sqrt{\bar{L}_x\bar{L}_y}}{\bar{L}_z}\right)^2\right],\Pi_{\dot{\gamma}_{xz}}=\left[\frac{\dot{\gamma}_{xz}\bar{L}_z}{V_z}\left(\frac{\bar{L}_x}{\bar{L}_z}\right)\right],\Pi_{\dot{\gamma}_{yz}}=\left[\frac{\dot{\gamma}_{yz}\bar{L}_z}{V_z}\left(\frac{\bar{L}_y}{\bar{L}_z}\right)\right]; \quad (7a\text{-}f)$$

- three displacement components

$$\Pi_{\delta_x}=\left[\frac{\delta_x}{\bar{L}_x}\left(\frac{\bar{L}_x}{\bar{L}_z}\right)^2\right],\Pi_{\delta_y}=.\left[\frac{\delta_y}{\bar{L}_y}\left(\frac{\bar{L}_y}{\bar{L}_z}\right)^2\right],\Pi_{\delta_z}=\left[\frac{\delta_z}{\bar{L}_z}\right]; \quad (8a\text{-}c)$$

- time

$$\Pi_t=\left[\frac{tV_z}{\bar{L}_z}\right]; \quad (9)$$

- mass

$$\Pi_M=\left[\frac{M}{\rho\bar{L}_x\bar{L}_y\bar{L}_z}\right],\Pi_G=\left[\frac{G}{\rho\bar{L}_x\bar{L}_y\bar{L}_z}\right]; \quad (10a,b)$$

- impulse pressure

Preprints (www.preprints.org) | NOT PEER-REVIEWED | Posted: 26 February 2020 doi:10.20944/preprints202002.0394.v1

$$\Pi_{P_z} = \left[\frac{P_z}{\rho V_z^2}\right]. \tag{11}$$

Firstly, the dimensionless numbers of stress and external loadings (Eqs.(5a-f), (10b), (11)) describe the most essential dynamic similarity of impact problems by the ratio of inertial loads (or impact loads) to the resistance of the structure itself: (1) The number Π_{σ_x} represents the ratio of the inertia moment $\left[\left(\rho\bar{L}_x\bar{L}_y\bar{L}_z\right)\left(\frac{V_z^2}{\bar{L}_z}\right)\right]\bar{L}_x$ to the structural dynamic bending moment $\left[\sigma_x\left(\bar{L}_y\bar{L}_z\right)\right]\bar{L}_z$, where the form $\left(\frac{V_z^2}{\bar{L}_z}\right)$ represents the characteristic acceleration (caused by impact velocity V_z) along the z-axis, the form $\left[\sigma_x\left(\bar{L}_y\bar{L}_z\right)\right]$ represents the membrane force along the x-axis, and the form $\left[\sigma_x\left(\bar{L}_y\bar{L}_z\right)\right]\bar{L}_z$ represents the bending moment caused by normal stress σ_x; (2) the number Π_{σ_y} represents the ratio of the inertia moment $\left[\left(\rho\bar{L}_x\bar{L}_y\bar{L}_z\right)\left(\frac{V_z^2}{\bar{L}_z}\right)\right]\bar{L}_y$ to the structural dynamic bending moment $\left[\sigma_y(\bar{L}_x\bar{L}_z)\right]\bar{L}_z$, where $\left[\sigma_y(\bar{L}_x\bar{L}_z)\right]$ and $\left[\sigma_y(\bar{L}_x\bar{L}_z)\right]\bar{L}_z$ represent the membrane force along the y-axis and the bending moment caused by normal stress σ_y, respectively; (3) the number Π_{σ_z} represents the ratio of the inertia force $\left[\left(\rho\bar{L}_x\bar{L}_y\bar{L}_z\right)\left(\frac{V_z^2}{\bar{L}_z}\right)\right]$ to the structural internal force $\left[\sigma_z\left(\bar{L}_x\bar{L}_y\right)\right]$ along the z-axis; (4) the number $\Pi_{\tau_{xy}}$ represents the ratio of the inertia torque $\left[\left(\rho\bar{L}_x\bar{L}_y\bar{L}_z\right)\left(\frac{V_z^2}{\bar{L}_z}\right)\right]\bar{L}_y$ to the structural dynamic torque $\left[\tau_{xy}\bar{L}_y\bar{L}_z\right]\bar{L}_z$; (5) the number $\Pi_{\tau_{xz}}$ represents the ratio of the inertia force $\left[\left(\rho\bar{L}_x\bar{L}_y\bar{L}_z\right)\left(\frac{V_z^2}{\bar{L}_z}\right)\right]$ to the structural dynamic shear force $\left[\tau_{xz}\left(\bar{L}_y\bar{L}_z\right)\right]$; (6) the number $\Pi_{\tau_{yz}}$ represents the ratio of the inertia force $\left[\left(\rho\bar{L}_x\bar{L}_y\bar{L}_z\right)\left(\frac{V_z^2}{\bar{L}_z}\right)\right]$ to the structural dynamic shear force $\left[\tau_{yz}(\bar{L}_x\bar{L}_z)\right]$; (7) the number Π_G represents the ratio of the impact mass G to the structural mass $\left(\rho\bar{L}_x\bar{L}_y\bar{L}_z\right)$; (8) the number Π_{P_z} represents the ratio of the external load $\left[P_z\left(\bar{L}_x\bar{L}_y\right)\right]$

Preprints (www.preprints.org) | NOT PEER-REVIEWED | Posted: 26 February 2020 doi:10.20944/preprints202002.0394.v1

to the structural inertia force $\left[\left(\rho\bar{L}_x\bar{L}_y\bar{L}_z\right)\left(\frac{V_z^2}{\bar{L}_z}\right)\right]$.

Secondly, the numbers $\Pi_{\sigma_x}-\Pi_{\tau_{yz}}$ (Eq.(5a-f)), the numbers $\Pi_{\varepsilon_x}-\Pi_{\gamma_{yz}}$ (Eq.(6a-f)), the numbers $\Pi_{\dot{\varepsilon}_x}-\Pi_{\dot{\gamma}_{yz}}$ (Eq.(7a-f)) and the numbers $\Pi_{\delta_x}-\Pi_{\delta_z}$ (Eq.(8a-c)) can be express as four tensor forms

$$\Pi_{\sigma_{ij}}=\left[\frac{\rho V_k^2}{\sigma_{ij}}\left(\frac{\bar{L}_i\bar{L}_j}{\bar{L}_k\bar{L}_k}\right)\right],\Pi_{\varepsilon_{ij}}=\left[\varepsilon_{ij}\left(\frac{\bar{L}_i\bar{L}_j}{\bar{L}_k\bar{L}_k}\right)\right],\Pi_{\dot{\varepsilon}_{ij}}=\left[\frac{\dot{\varepsilon}_{ij}\bar{L}_k}{V_k}\left(\frac{\bar{L}_i\bar{L}_j}{\bar{L}_k\bar{L}_k}\right)\right]\ \text{and}$$
$$\Pi_{\delta_i}=\left[\frac{\delta_i}{\bar{L}_i}\left(\frac{\bar{L}_i\bar{L}_j}{\bar{L}_k\bar{L}_k}\right)\right]\left(no\ sum\ on\ i,j,k\right), \tag{12a-d}$$

where σ_{ij}, ε_{ij}, $\dot{\varepsilon}_{ij}$ and δ_i represent stress tensor, strain tensor, strain-rate tensor and displacement vector, respectively; $\bar{L}_i$, $\bar{L}_j$ and $\bar{L}_k$ are three orthogonal characteristic lengths of structure in cartesian coordinate system; $i,j=1,2,3\ (or\ x,y,z)$, $k=3\ (or\ z)$.

Thirdly, three spatial directions and structural geometric characteristics are explicitly expressed in these dimensionless numbers by the use of oriented characteristic lengths $\bar{L}_x$, $\bar{L}_y$ and $\bar{L}_z$, which remedy the defects of previous scalar dimensionless system (i.e., MLT, VSG, DLV, VSM, etc.).

Finally, these numbers (Eqs.(5)-(11)) all can be regard as the extension from pervious DLV numbers after further considering spatial directions. For example, the DLV numbers $\frac{\rho V^2}{\sigma}$, $\frac{\rho\bar{L}^2V^2}{F(\sigma)}$ and $\frac{\rho\bar{L}^3V^2}{\Psi(\sigma)}$ for stress σ are extended to the number $\Pi_{\sigma_{ij}}=\frac{\rho V_k^2}{\sigma_{ij}}\left(\frac{\bar{L}_i\bar{L}_j}{\bar{L}_k\bar{L}_k}\right)$ for stress tensor σ_{ij}; the DLV number $\frac{\delta}{\bar{L}}$ for displacement δ is extended to the number $\Pi_{\delta_i}=\frac{\delta_i}{\bar{L}_i}\left(\frac{\bar{L}_i\bar{L}_j}{\bar{L}_k\bar{L}_k}\right)$ for displacement vector δ_i; the DLV number $\frac{G}{\rho\bar{L}^3}$ for impact mass G is extended to the number $\Pi_G=\frac{G}{\rho\bar{L}_x\bar{L}_y\bar{L}_z}$. Since the above analysis based on oriented-density-length-velocity dimensional analysis, these new proposed

Preprints (www.preprints.org) | NOT PEER-REVIEWED | Posted: 26 February 2020 doi:10.20944/preprints202002.0394.v1

dimensionless numbers can be termed as the ODLV system (or the oriented-DLV system) in the following sections.

2.3. Dimensionless expression for equivalent stress, equivalent strain and equivalent strain rate

For structure subjected to impact loading, the similarity law of the equivalent stress σ_{eq}, the equivalent strain ε_{eq} and the equivalent strain rate $\dot{\varepsilon}_{eq}$ needs to be further considered.

Considering the assumptions $\tau_{xz}=\tau_{yz}=\sigma_z=0$ and $\gamma_{xz}=\gamma_{yz}=\varepsilon_z=0$ for the thin-plate problem in Sect. 2.1, σ_{eq}, ε_{eq} and $\dot{\varepsilon}_{eq}$ (Yu and Xue, 2010) can be simplified as

$$\begin{aligned}\sigma_{eq}&=\frac{1}{\sqrt{2}}\sqrt{\left(\sigma_x-\sigma_y\right)^2+\left(\sigma_y-\sigma_z\right)^2+\left(\sigma_z-\sigma_x\right)^2+6\left(\tau_{xy}^2+\tau_{yz}^2+\tau_{zx}^2\right)}\\&=\sqrt{\sigma_x^2+\sigma_y^2-\sigma_x\sigma_y+3\tau_{xy}^2},\end{aligned}\tag{13}$$

$$\begin{aligned}\varepsilon_{eq}&=\frac{\sqrt{2}}{3}\sqrt{\left(\varepsilon_x-\varepsilon_y\right)^2+\left(\varepsilon_y-\varepsilon_z\right)^2+\left(\varepsilon_x-\varepsilon_z\right)^2+6\left(\gamma_{xy}^2+\gamma_{xz}^2+\gamma_{yz}^2\right)}\\&=\frac{2}{3}\sqrt{\varepsilon_x^2+\varepsilon_y^2-\varepsilon_x\varepsilon_y+3\gamma_{xy}^2}\end{aligned}\tag{14}$$

and

$$\dot{\varepsilon}_{eq}=\frac{2}{3}\sqrt{\dot{\varepsilon}_x^2+\dot{\varepsilon}_y^2-\dot{\varepsilon}_x\dot{\varepsilon}_y+3\dot{\gamma}_{xy}^2},\tag{15}$$

respectively.

The oriented dimensional analysis for Eqs. (13)-(15) indicates three dimension's relations as

$$\dim\left(\sigma_{eq}\right)=\dim\left(\sigma_x\right)=\dim\left(\sigma_y\right)=\dim\left(\sqrt{\sigma_x\sigma_y}\right)=\dim\left(\tau_{xy}\right),\tag{16}$$

Preprints (www.preprints.org) | NOT PEER-REVIEWED | Posted: 26 February 2020 doi:10.20944/preprints202002.0394.v1

$$\dim\left(\varepsilon_{eq}\right)=\dim\left(\varepsilon_{x}\right)=\dim\left(\varepsilon_{y}\right)=\dim\left(\sqrt{\varepsilon_{x}\varepsilon_{y}}\right)=\dim\left(\gamma_{xy}\right) \tag{17}$$

and

$$\dim\left(\dot{\varepsilon}_{eq}\right)=\dim\left(\dot{\varepsilon}_{x}\right)=\dim\left(\dot{\varepsilon}_{y}\right)=\dim\left(\sqrt{\dot{\varepsilon}_{x}\dot{\varepsilon}_{y}}\right)=\dim\left(\dot{\gamma}_{xy}\right), \tag{18}$$

respectively.

When substituting the dimensions of stress components σ_x, σ_y and σ_z (Table 3) into Eqs. (16)-(18), one obtains

$$\dim\left(\sigma_{eq}\right)=\mathbb{L}_{x}\mathbb{L}_{y}^{-1}\mathbb{L}_{z}^{-1}\mathbb{M}\mathbb{T}^{-2}=\mathbb{L}_{x}^{-1}\mathbb{L}_{y}\mathbb{L}_{z}^{-1}\mathbb{M}\mathbb{T}^{-2}=\mathbb{L}_{z}^{-1}\mathbb{M}\mathbb{T}^{-2}=\mathbb{L}_{z}^{-1}\mathbb{M}\mathbb{T}^{-2}, \tag{19}$$

$$\dim\left(\varepsilon_{eq}\right)=\mathbb{L}_{x}^{-2}\mathbb{L}_{z}^{2}=\mathbb{L}_{y}^{-2}\mathbb{L}_{z}^{2}=\mathbb{L}_{x}^{-1}\mathbb{L}_{y}^{-1}\mathbb{L}_{z}^{2}=\mathbb{L}_{x}^{-1}\mathbb{L}_{y}^{-1}\mathbb{L}_{z}^{2} \tag{20}$$

and

$$\dim\left(\dot{\varepsilon}_{eq}\right)=\mathbb{L}_{x}^{-2}\mathbb{L}_{z}^{2}\mathbb{T}^{-1}=\mathbb{L}_{y}^{-2}\mathbb{L}_{z}^{2}\mathbb{T}^{-1}=\mathbb{L}_{x}^{-1}\mathbb{L}_{y}^{-1}\mathbb{L}_{z}^{2}\mathbb{T}^{-1}=\mathbb{L}_{x}^{-1}\mathbb{L}_{y}^{-1}\mathbb{L}_{z}^{2}\mathbb{T}^{-1}, \tag{21}$$

respectively.

The establishment condition of Eqs. (19)-(21) is $\mathbb{L}_x \triangleq \mathbb{L}_y$, which means the dimension $\mathbb{L}_x$ and the dimension $\mathbb{L}_y$ are not independent. In this equality, the operator '$\triangleq$' is a defined sign of equality in which the directions of characteristic lengths in the x-y plane on both sides of the equation are not distinguished. Therefore, for the equivalent stress, strain and strain rate, the directions of the x-y plane are isotropic. In order to better describe this phenomenon, the notation $\mathbb{L}_{xy}=\sqrt{\mathbb{L}_x\mathbb{L}_y}$ can be used instead of the length dimension of the x-y plane, where $\mathbb{L}_x\mathbb{L}_y$ represents the dimension of area in the x-y plane; and the constraint relation $\mathbb{L}_x \triangleq \mathbb{L}_y$ can be expressed as the number $\Pi_{x-y}=\frac{\bar{L}_x}{\bar{L}_y}$, which means that the different directions of the x-y plane follow the same law of similarity.

When using the dimensional analysis of ODLV to express physical quantities σ_{eq},

Preprints (www.preprints.org) | NOT PEER-REVIEWED | Posted: 26 February 2020 doi:10.20944/preprints202002.0394.v1

ε_{eq} and $\dot{\varepsilon}_{eq}$, three dimensionless numbers can be obtained as follows:

$$\Pi_{\sigma_{eq}}=\left[\frac{\rho V_z^2}{\sigma_{eq}}\left(\frac{\bar{L}_{xy}}{\bar{L}_z}\right)^2\right],\Pi_{\varepsilon_{eq}}=\left[\varepsilon_{eq}\left(\frac{\bar{L}_{xy}}{\bar{L}_z}\right)^2\right],\Pi_{\dot{\varepsilon}_{eq}}=\left[\frac{\dot{\varepsilon}_{eq}\bar{L}_z}{V_z}\left(\frac{\bar{L}_{xy}}{\bar{L}_z}\right)^2\right], \tag{22a-c}$$

where $\bar{L}_{xy}$ represents the characteristic length of the x-y plane. It can be learn from the above analysis that the number $\Pi_{\sigma_{eq}}$, the number $\Pi_{\varepsilon_{eq}}$ and the number $\Pi_{\dot{\varepsilon}_{eq}}$ can be regard as the derivation forms for the isotropic x-y plane from the numbers Π_{σ_x}, Π_{σ_y}, $\Pi_{\tau_{xy}}$, the numbers Π_{ε_x}, Π_{ε_y}, $\Pi_{\gamma_{xy}}$ and the numbers $\Pi_{\dot{\varepsilon}_x}$, $\Pi_{\dot{\varepsilon}_y}$, $\Pi_{\dot{\gamma}_{yz}}$, respectively.

In what follows, the oriented dimension analysis for the relationships between stress components and strain components will be derived by the constitutive relation of the plastic increment theory.

In order to simplify the study, we consider only the plastic stress and strain (i.e., ignoring the elastic part) and the rigid-perfectly plastic materials. Then the $Lévy-Mises$ theory (Yu and Xue, 2010) is adopted as

$$\left.\begin{aligned}
d\varepsilon_x&=\frac{d\varepsilon_{eq}}{\sigma_{eq}}\left[\sigma_x-\frac{1}{2}\left(\sigma_y+\sigma_z\right)\right]\\
d\varepsilon_y&=\frac{d\varepsilon_{eq}}{\sigma_{eq}}\left[\sigma_y-\frac{1}{2}\left(\sigma_x+\sigma_z\right)\right]\\
d\varepsilon_z&=\frac{d\varepsilon_{eq}}{\sigma_{eq}}\left[\sigma_z-\frac{1}{2}\left(\sigma_x+\sigma_y\right)\right]\\
d\varepsilon_{xy}&=\frac{3}{2}\frac{d\varepsilon_{eq}}{\sigma_{eq}}\tau_{xy}\\
d\varepsilon_{yz}&=\frac{3}{2}\frac{d\varepsilon_{eq}}{\sigma_{eq}}\tau_{yz}\\
d\varepsilon_{xz}&=\frac{3}{2}\frac{d\varepsilon_{eq}}{\sigma_{eq}}\tau_{xz}
\end{aligned}\right\}, \tag{23a-f}$$

where $d\varepsilon_x, d\varepsilon_y, d\varepsilon_z, d\gamma_{xy}, d\gamma_{xz}, d\gamma_{xz}$ are six plastic strain increments; $d\varepsilon_{eq}=$

Preprints (www.preprints.org) | NOT PEER-REVIEWED | Posted: 26 February 2020 doi:10.20944/preprints202002.0394.v1

$\frac{\sqrt{2}}{3}\left[\left(d\varepsilon_x - d\varepsilon_y\right)^2 + \left(d\varepsilon_y - d\varepsilon_z\right)^2 + (d\varepsilon_z - d\varepsilon_x)^2 + \frac{3}{2}\left(d\gamma_{xy}^2 + d\gamma_{yz}^2 + d\gamma_{zy}^2\right)\right]^{1/2}$ is the equivalent plastic strain increment.

When the stress component σ_z is ignored, the oriented dimensional analysis for Eq. (23a-f) will leads to the following relations

$$\left.\begin{aligned}
\dim(\varepsilon_x) &= \frac{\dim(\varepsilon_{eq})}{\dim(\sigma_{eq})}\dim(\sigma_x) = \frac{\dim(\varepsilon_{eq})}{\dim(\sigma_{eq})}\dim(\sigma_y) \\
\dim(\varepsilon_y) &= \frac{\dim(\varepsilon_{eq})}{\dim(\sigma_{eq})}\dim(\sigma_y) = \frac{\dim(\varepsilon_{eq})}{\dim(\sigma_{eq})}\dim(\sigma_x) \\
\dim(\varepsilon_z) &= \frac{\dim(\varepsilon_{eq})}{\dim(\sigma_{eq})}\dim(\sigma_x) = \frac{\dim(\varepsilon_{eq})}{\dim(\sigma_{eq})}\dim(\sigma_y) \\
\dim(\varepsilon_{xy}) &= \frac{\dim(\varepsilon_{eq})}{\dim(\sigma_{eq})}\dim(\tau_{xy}) \\
\dim(\varepsilon_{yz}) &= \frac{\dim(\varepsilon_{eq})}{\dim(\sigma_{eq})}\dim(\tau_{yz}) \\
\dim(\varepsilon_{xz}) &= \frac{\dim(\varepsilon_{eq})}{\dim(\sigma_{eq})}\dim(\tau_{xz})
\end{aligned}\right\}, \qquad \text{(24a-f)}$$

respectively.

It is obvious that when the dimensions of ε_x, ε_y, ε_{xy}, σ_x, σ_y, τ_{xy}, σ_{eq}, ε_{eq} (Table 3; Eqs. (19) and (20)) are substituted, for the isotropic x-y plane, Eq. (24a,b,d) is automatically satisfied. While, when the dimensions of σ_x, σ_y, τ_{xz}, τ_{yz}, σ_{eq}, ε_{eq} (Table 3; Eqs. (19) and (20)) are substituted, for the isotropic x-y plane, Eq. (24c,e,f) derives the modified dimension of strain components ε_z, γ_{yz}, γ_{xz} as

Preprints (www.preprints.org) | NOT PEER-REVIEWED | Posted: 26 February 2020 doi:10.20944/preprints202002.0394.v1

$$\left.\begin{aligned}\dim\left(\varepsilon_z\right)&=\dim\left(\varepsilon_{eq}\right)=\mathbb{L}_{xy}^{-2}\mathbb{L}_z^2\\ \dim\left(\varepsilon_{yz}\right)&=\frac{\dim\left(\tau_{yz}\right)}{\dim\left(\sigma_{eq}\right)}\dim\left(\varepsilon_{eq}\right)=\mathbb{L}_{xy}^{-3}\mathbb{L}_z^3\\ \dim\left(\varepsilon_{xz}\right)&=\frac{\dim\left(\tau_{xz}\right)}{\dim\left(\sigma_{eq}\right)}\dim\left(\varepsilon_{eq}\right)=\mathbb{L}_{xy}^{-3}\mathbb{L}_z^3\end{aligned}\right\},\qquad(25a\text{-}c)$$

which is different form the oriented dimension in Table 3. Since the modified dimension of ε_z is consistent with the dimension of ε_{eq}, the equivalent strain can further consider as $\varepsilon_{eq}=\frac{\sqrt{2}}{3}\sqrt{\left(\varepsilon_x-\varepsilon_y\right)^2+\left(\varepsilon_y-\varepsilon_z\right)^2+(\varepsilon_x-\varepsilon_z)^2+6\gamma_{xy}^2}$ for the derivation of the thin-plate problem. Accordingly, the equivalent strain rate $\dot{\varepsilon}_{eq}$ can also take the effect of strain rate component $\dot{\varepsilon}_z$ into further consideration. In addition, the three modified dimensions can also be obtained from the oriented analysis for the bending strains of ε_z, γ_{xz}, γ_{yz}. For a beam under the Euler—Bernoulli kinematic hypothesis, the only nonzero, nonlinear strain components are expressed $\varepsilon_z=\frac{1}{2}\left(\frac{\partial w}{\partial x}\right)^2$ and $\gamma_{xz}=\left(-\frac{\partial u}{\partial x}\frac{\partial w}{\partial x}\right)+\left(Z\frac{\partial^2 w}{\partial x^2}\frac{\partial w}{\partial x}\right)$ (Reddy., 2007). The dimension of ε_z can be modified as $\mathbb{L}_x^{-2}\mathbb{L}_z^2$ through the oriented dimension analysis $dim\left(\left(\frac{\partial w}{\partial x}\right)^2\right)=\mathbb{L}_x^{-2}\mathbb{L}_z^2$ for the definition $\varepsilon_z=\frac{1}{2}\left(\frac{\partial w}{\partial x}\right)^2$; the dimension of γ_{xz} can be modified as $\mathbb{L}_x^{-3}\mathbb{L}_z^3$ through the oriented dimension analysis $dim\left(\frac{\partial u}{\partial x}\frac{\partial w}{\partial x}\right)=dim\left(Z\frac{\partial^2 w}{\partial x^2}\frac{\partial w}{\partial x}\right)=\mathbb{L}_x^{-3}\mathbb{L}_z^3$ for the definition $\gamma_{xz}=\left(-\frac{\partial u}{\partial x}\frac{\partial w}{\partial x}\right)+\left(Z\frac{\partial^2 w}{\partial x^2}\frac{\partial w}{\partial x}\right)$. Obviously, these dimensions are consistent with Eq. (25a,c).

Based on the three modified dimensions, the numbers Π_{ε_z}, $\Pi_{\gamma_{xz}}$, $\Pi_{\gamma_{yz}}$, $\Pi_{\dot{\varepsilon}_z}$, $\Pi_{\dot{\gamma}_{xz}}$ and $\Pi_{\dot{\gamma}_{yz}}$ are modified accordingly as

Preprints (www.preprints.org) | NOT PEER-REVIEWED | Posted: 26 February 2020 doi:10.20944/preprints202002.0394.v1

$$\Pi_{\varepsilon_z}^{\mathrm{mod}}=\left[\varepsilon_z\left(\frac{\bar{L}_{xy}}{\bar{L}_z}\right)^2\right],\Pi_{\gamma_{xz}}^{\mathrm{mod}}=\left[\gamma_{xz}\left(\frac{\bar{L}_{xy}}{\bar{L}_z}\right)^3\right],\Pi_{\gamma_{yz}}^{\mathrm{mod}}=\left[\gamma_{yz}\left(\frac{\bar{L}_{xy}}{\bar{L}_z}\right)^3\right],$$
$$\Pi_{\dot{\varepsilon}_z}^{\mathrm{mod}}=\left[\frac{\dot{\varepsilon}_z L_z}{V_z}\left(\frac{\bar{L}_{xy}}{\bar{L}_z}\right)^2\right],\Pi_{\dot{\gamma}_{xz}}^{\mathrm{mod}}=\left[\frac{\dot{\gamma}_{xz}\bar{L}_z}{V_z}\left(\frac{\bar{L}_{xy}}{\bar{L}_z}\right)^3\right],\Pi_{\dot{\gamma}_{yz}}^{\mathrm{mod}}=\left[\frac{\dot{\gamma}_{yz}\bar{L}_z}{V_z}\left(\frac{\bar{L}_{xy}}{\bar{L}_z}\right)^3\right], \quad (26a\text{-}f)$$

where the superscript 'mod' represents modification for physical quantity. The difference between the numbers $\Pi_{\varepsilon_z}^{mod}$- $\Pi_{\dot{\gamma}_{yz}}^{mod}$ (Eq.(26a-f)) and the numbers Π_{ε_z}, $\Pi_{\gamma_{xz}}$, $\Pi_{\gamma_{yz}}$, $\Pi_{\dot{\varepsilon}_z}$, $\Pi_{\dot{\gamma}_{xz}}$, $\Pi_{\dot{\gamma}_{yz}}$ (Eqs. (6c,e,f) and (7c,e,f)) comes from the effect of plastic yield on material deformation.

It is evident from the above analysis that the dimensionless expression for the equivalent stress, strain and strain rate has plentiful physical implications. (1) The number $\Pi_{\sigma_{eq}}=\frac{\rho V_z^2}{\sigma_{eq}}\left(\frac{\bar{L}_{xy}}{\bar{L}_z}\right)^2$ is in full accord with the Zhao's response number $R_n(n=2)=\frac{\rho V_0^2}{\sigma_0}\left(\frac{\bar{L}}{H}\right)^2$ when substituting σ_{eq} as σ_0. Therefore, it has the ability to measure the response of impacted structures. (2) Since the membrane force, bending moment and in-plane torque for the x-y plane are determined by stress components σ_x, σ_y, τ_{xy}, the number $\Pi_{\sigma_{eq}}$ have already contains the dimensionless causal relationship between these forces and equivalent stress σ_{eq}, i.e. $\Pi_{\sigma_x}\triangleq\Pi_{\sigma_y}\triangleq\Pi_{\tau_{xy}}\triangleq\Pi_{\sigma_{eq}}$. Therefore, the number $\Pi_{\sigma_{eq}}$ reflects the most essential dynamic similarity for the isotropic x-y plane by the ratio of the inertia force (or bending moment; or torque) $\left[\left(\rho\bar{L}_{xy}^2\bar{L}_z\right)\left(\frac{V_z^2}{\bar{L}_z}\right)\right]\bar{L}_{xy}$ to the characteristic of the fully plastic membrane force (or bending moment; or torque) $\left[\sigma_d\left(\bar{L}_{xy}\bar{L}_z\right)\right]\bar{L}_z$. (3) The derivation for $\Pi_{\sigma_{eq}}$ also explains the difference between the Johnson's damage number D_n and the Zhao's response number R_n from the view of point of oriented dimensional analysis. The oriented dimension analysis $dim(\sigma_{eq})=dim(\sigma_{ij})=\mathbb{LMT}^{-2}$ for the equivalent stress

Preprints (www.preprints.org) | NOT PEER-REVIEWED | Posted: 26 February 2020 doi:10.20944/preprints202002.0394.v1

considering six stress components will derive the number $\Pi_{\sigma_{eq}} = \frac{\rho V_z^2}{\sigma_{eq}}$, which is in full accord with the Johnson's damage number D_n. This indicates that the damage number is the dimensionless expression for equivalent stress following the same similarity laws in three geometric directions, while the response number is the dimensionless expression for equivalent stress following the same similarity laws only in the x-y plane. (4) The effect of structure geometry exists not only in the numbers of stress, strain and strain rate components (Eqs. (5-7) and (26)) but also in the numbers of equivalent stress, strain and strain rete (Eq. (22)), which usually expressed by the ratio of characteristic lengths in two different directions. And the different power exponents of ratios indicate these dimensionless numbers follow different geometric similarity laws. (5) The characteristic length $\bar{L}_z$ and the characteristic length $\bar{L}_{xy}$ are independent of each other in the thin-plate problem, which will be the foundation for the geometric distortion of thickness in the following content.

2.4. Scaling factors

The structural similarity means these dimensionless numbers are complete equality between scaled model and prototype, which can be used to derive scaling factors of physical quantity. For example, the equation $\left(\Pi_{\sigma_x}\right)_m = \left(\Pi_{\sigma_x}\right)_p$ leads to

$$\frac{\rho_m \left(V_z\right)_m^2}{\left(\sigma_x\right)_m}\left[\frac{\left(\bar{L}_x\right)_m}{\left(\bar{L}_z\right)_m}\right]^2 = \frac{\rho_p \left(V_z\right)_p^2}{\left(\sigma_x\right)_p}\left[\frac{\left(\bar{L}_x\right)_p}{\left(\bar{L}_z\right)_p}\right]^2 \rightarrow \beta_{\sigma_x} = \beta_\rho \beta_{V_z}^2 \left(\beta_{\bar{L}_x} / \beta_{\bar{L}_z}\right)^2. \qquad (27)$$

Similarly, other dimensionless numbers (Eqs. (5)-(11), (22), (26)) can obtain their corresponding scaling factors. These scaling factors are listed in Table 4.

Preprints (www.preprints.org) | NOT PEER-REVIEWED | Posted: 26 February 2020 doi:10.20944/preprints202002.0394.v1

Table 4 Main scaling factors of structural impact in the ODLV system.

Variable	Scaling factor	Variable	Scaling factor
Length $\bar{L}_x$	$\beta_{\bar{L}_x} = (\bar{L}_x)_m/(\bar{L}_x)_p$	Strain rate $\dot{\varepsilon}_z$	$\beta_{\dot{\varepsilon}_z} = (\beta_{V_z}/\beta_{\bar{L}_z})$
Length $\bar{L}_y$	$\beta_{\bar{L}_y} = (\bar{L}_y)_m/(\bar{L}_y)_p$	Strain rate $\dot{\gamma}_{xy}$	$\beta_{\dot{\gamma}_{xy}} = (\beta_{V_z}/\beta_{\bar{L}_z})\left(\beta_{\bar{L}_z}/\sqrt{\beta_{\bar{L}_x}\beta_{\bar{L}_y}}\right)^2$
Length $\bar{L}_z$	$\beta_{\bar{L}_z} = (\bar{L}_z)_m/(\bar{L}_z)_p$	Strain rate $\dot{\gamma}_{xz}$	$\beta_{\dot{\gamma}_{xz}} = (\beta_{V_z}/\beta_{\bar{L}_z})(\beta_{\bar{L}_z}/\beta_{\bar{L}_x})$
Density ρ	$\beta_\rho = \rho_m/\rho_p$	Strain rate $\dot{\gamma}_{yz}$	$\beta_{\dot{\gamma}_{yz}} = (\beta_{V_z}/\beta_{\bar{L}_z})\left(\beta_{\bar{L}_z}/\beta_{\bar{L}_y}\right)$
Velocity V_z	$\beta_{V_z} = (V_z)_m/(V_z)_p$	Time t	$\beta_t = \left(\beta_{\bar{L}_z}/\beta_{V_z}\right)$
Normal stress σ_x	$\beta_{\sigma_x} = (\beta_\rho\beta_{V_z}^2)(\beta_{\bar{L}_x}/\beta_{\bar{L}_z})^2$	Displacement δ_x	$\beta_{\delta_x} = \beta_{\bar{L}_x}(\beta_{\bar{L}_z}/\beta_{\bar{L}_x})^2$
Normal stress σ_y	$\beta_{\sigma_y} = (\beta_\rho\beta_{V_z}^2)\left(\beta_{\bar{L}_y}/\beta_{\bar{L}_z}\right)^2$	Displacement δ_y	$\beta_{\delta_y} = \beta_{\bar{L}_y}\left(\beta_{\bar{L}_z}/\beta_{\bar{L}_y}\right)^2$
Normal stress σ_z	$\beta_{\sigma_z} = (\beta_\rho\beta_{V_z}^2)$	Displacement δ_z	$\beta_{\delta_z} = \beta_{\bar{L}_z}$
Shear stress τ_{xy}	$\beta_{\tau_{xy}} = (\beta_\rho\beta_{V_z}^2)\left(\sqrt{\beta_{\bar{L}_x}\beta_{\bar{L}_y}}/\beta_{\bar{L}_z}\right)^2$	Mass M, G	$\beta_M = \beta_G = \beta_\rho\left(\beta_{\bar{L}_x}\beta_{\bar{L}_y}\beta_{\bar{L}_z}\right)$
Shear stress τ_{xz}	$\beta_{\tau_{xz}} = (\beta_\rho\beta_{V_z}^2)(\beta_{\bar{L}_x}/\beta_{\bar{L}_z})$	Surface pressure P_z	$\beta_{P_z} = (\beta_\rho\beta_{V_z}^2)$
Shear stress τ_{yz}	$\beta_{\tau_{yz}} = (\beta_\rho\beta_{V_z}^2)\left(\beta_{\bar{L}_y}/\beta_{\bar{L}_z}\right)$	Equivalent stress σ_{eq}	$\beta_{\sigma_{eq}} = (\beta_\rho\beta_{V_z}^2)\left(\beta_{\bar{L}_{xy}}/\beta_{\bar{L}_z}\right)^2$
Normal strain ε_x	$\beta_{\varepsilon_x} = \left(\beta_{\bar{L}_z}/\beta_{\bar{L}_x}\right)^2$	Equivalent strain ε_{eq}	$\beta_{\varepsilon_{eq}} = \left(\beta_{\bar{L}_z}/\beta_{\bar{L}_{xy}}\right)^2$
Normal strain ε_y	$\beta_{\varepsilon_y} = \left(\beta_{\bar{L}_z}/\beta_{\bar{L}_y}\right)^2$	Equivalent strain rate $\dot{\varepsilon}_{eq}$	$\beta_{\dot{\varepsilon}_{eq}} = (\beta_{V_z}/\beta_{\bar{L}_z})\left(\beta_{\bar{L}_z}/\beta_{\bar{L}_{xy}}\right)^2$
Normal strain ε_z	$\beta_{\varepsilon_z} = 1$	Normal strain ε_z	$\beta_{\varepsilon_z}^{mod} = \left(\beta_{\bar{L}_z}/\beta_{\bar{L}_{xy}}\right)^2$
Shear strain γ_{xy}	$\beta_{\gamma_{xy}} = \left(\beta_{\bar{L}_z}/\sqrt{\beta_{\bar{L}_x}\beta_{\bar{L}_y}}\right)^2$	Shear strain γ_{xz}	$\beta_{\gamma_{xz}}^{mod} = \left(\beta_{\bar{L}_z}/\beta_{\bar{L}_{xy}}\right)^3$
Shear strain γ_{xz}	$\beta_{\gamma_{xz}} = (\beta_{\bar{L}_z}/\beta_{\bar{L}_x})$	Shear strain γ_{yz}	$\beta_{\gamma_{yz}}^{mod} = \left(\beta_{\bar{L}_z}/\beta_{\bar{L}_{xy}}\right)^3$
Shear strain γ_{yz}	$\beta_{\gamma_{yz}} = \left(\beta_{\bar{L}_z}/\beta_{\bar{L}_y}\right)$	Strain rate $\dot{\varepsilon}_z$	$\beta_{\dot{\varepsilon}_z}^{mod} = (\beta_{V_z}/\beta_{\bar{L}_z})\left(\beta_{\bar{L}_z}/\beta_{\bar{L}_{xy}}\right)^2$
Strain rate $\dot{\varepsilon}_x$	$\beta_{\dot{\varepsilon}_x} = (\beta_{V_z}/\beta_{\bar{L}_z})(\beta_{\bar{L}_z}/\beta_{\bar{L}_x})^2$	Strain rate $\dot{\gamma}_{xz}$	$\beta_{\dot{\gamma}_{xz}}^{mod} = (\beta_{V_z}/\beta_{\bar{L}_z})\left(\beta_{\bar{L}_z}/\beta_{\bar{L}_{xy}}\right)^3$
Strain rate $\dot{\varepsilon}_y$	$\beta_{\dot{\varepsilon}_y} = (\beta_{V_z}/\beta_{\bar{L}_z})\left(\beta_{\bar{L}_z}/\beta_{\bar{L}_y}\right)^2$	Strain rate $\dot{\gamma}_{yz}$	$\beta_{\dot{\gamma}_{yz}}^{mod} = (\beta_{V_z}/\beta_{\bar{L}_z})\left(\beta_{\bar{L}_z}/\beta_{\bar{L}_{xy}}\right)^3$

It can be seen from Table 4 that the scaling factors of physical quantities are

Preprints (www.preprints.org) | NOT PEER-REVIEWED | Posted: 26 February 2020 doi:10.20944/preprints202002.0394.v1

directly expressed by the five basic scaling factors β_ρ, $\beta_{\bar{L}_x}$, $\beta_{\bar{L}_y}$, $\beta_{\bar{L}_z}$ and β_{V_z}. For other physical quantities, their scaling factor can be derived from their physical definitions; for instance, $\beta_{V_x} = \beta_{V_z}(\beta_{\bar{L}_z}/\beta_{\bar{L}_x})$ can be obtained by the substation of the factors $\beta_{\delta_x} = \beta_{\bar{L}_x}(\beta_{\bar{L}_z}/\beta_{\bar{L}_x})^2$ and $\beta_t = (\beta_{\bar{L}_z}/\beta_{V_z})$ into the factor $\beta_{V_x} = \beta_{\delta_x}/\beta_t$; $\beta_{F_x} = (\beta_\rho \beta_{V_z}^2)\left(\beta_{\bar{L}_y}\beta_{\bar{L}_z}\right)(\beta_{\bar{L}_x}/\beta_{\bar{L}_z})^2$ can be obtained by the substation of the factors $\beta_{\sigma_x} = (\beta_\rho \beta_{V_z}^2)(\beta_{\bar{L}_x}/\beta_{\bar{L}_z})^2$ into the factor $\beta_{F_x} = \beta_{\sigma_x}\left(\beta_{\bar{L}_y}\beta_{\bar{L}_z}\right)$. In addition, compared with the VSG factors (Table 1), the five basic factors β_ρ, $\beta_{\bar{L}_x}$, $\beta_{\bar{L}_y}$, $\beta_{\bar{L}_z}$ and β_{V_z} can be considered as the direct extension for three basic factors $\beta_{\bar{L}}$, β_V and β_ρ after considering three spatial directions. Therefore, the ODLV system includes the same addressing ability for the material distortion with the VSG system. Compared with the VSM factors (Table 2), the factors of stress, strain, strain rate, displacement, and so on are reasonably modified.

2.5. Application of scaling factors on the constitutive equation

Based on the factor $\beta_{\sigma_{eq}}$, $\beta_{\varepsilon_{eq}}$ and $\beta_{\dot{\varepsilon}_{eq}}$ of Table 4, the non-scaling problems of structural impact can be addressed by reasonably correcting the input parameters of scaled model.

From the view of point of plastic mechanics, three basic physical quantities σ_d, ε and $\dot{\varepsilon}$ for the material constitutive equation $\sigma_d = f(\varepsilon, \dot{\varepsilon})$ are often substituted by σ_{eq}, ε_{eq} and $\dot{\varepsilon}_{eq}$, respectively. Then, the substitution of $\beta_{\sigma_{eq}} = (\beta_\rho \beta_{V_z}^2)\left(\beta_{\bar{L}_{xy}}/\beta_{\bar{L}_z}\right)^2$, $\beta_{\varepsilon_{eq}} = \left(\beta_{\bar{L}_z}/\beta_{\bar{L}_{xy}}\right)^2$ and $\beta_{\dot{\varepsilon}_{eq}} = (\beta_{V_z}/\beta_{\bar{L}_z})\left(\beta_{\bar{L}_z}/\beta_{\bar{L}_{xy}}\right)^2$ into the constitutive equation of scaled model (i.e., $(\sigma_d)_m = f_m(\varepsilon_m, \dot{\varepsilon}_m)$) obtains the predicted dynamic flow stress

Preprints (www.preprints.org) | NOT PEER-REVIEWED | Posted: 26 February 2020 doi:10.20944/preprints202002.0394.v1

$$\begin{aligned}\left(\sigma_d\right)_p^{predicted} &= \left(\sigma_{eq}\right)_m / \beta_{\sigma_{eq}} = f_m\left(\left(\varepsilon_{eq}\right)_m, \left(\dot{\varepsilon}_{eq}\right)_m\right) \frac{1}{\beta_\rho \beta_{V_z}^2} \left(\frac{\beta_{\bar{L}_z}}{\beta_{\bar{L}_{xy}}}\right)^2 \\ &= f_m\left\{\left(\varepsilon_{eq}\right)_p \left(\frac{\beta_{\bar{L}_z}}{\beta_{\bar{L}_{xy}}}\right)^2, \left(\dot{\varepsilon}_{eq}\right)_p \frac{\beta_{V_z}}{\beta_{\bar{L}_z}} \left(\frac{\beta_{\bar{L}_z}}{\beta_{\bar{L}_{xy}}}\right)^2\right\} \frac{1}{\beta_\rho \beta_{V_z}^2} \left(\frac{\beta_{\bar{L}_z}}{\beta_{\bar{L}_{xy}}}\right)^2\end{aligned} \tag{28}$$

by the scaled model.

The similarity laws require $(\sigma_d)_p^{predicted} = (\sigma_d)_p = f_p\left(\left(\varepsilon_{eq}\right)_p, \left(\dot{\varepsilon}_{eq}\right)_p\right)$, i.e.

$$f_m\left\{\left(\varepsilon_{eq}\right)_p \left(\frac{\beta_{\bar{L}_z}}{\beta_{\bar{L}_{xy}}}\right)^2, \left(\dot{\varepsilon}_{eq}\right)_p \frac{\beta_{V_z}}{\beta_{\bar{L}_z}} \left(\frac{\beta_{\bar{L}_z}}{\beta_{\bar{L}_{xy}}}\right)^2\right\} \frac{1}{\beta_\rho \beta_{V_z}^2} \left(\frac{\beta_{\bar{L}_z}}{\beta_{\bar{L}_{xy}}}\right)^2 = f_p\left\{\left(\varepsilon_{eq}\right)_p, \left(\dot{\varepsilon}_{eq}\right)_p\right\}, \tag{29}$$

which gives a functional relation among four factors β_ρ, $\beta_{\bar{L}_{xy}}$, $\beta_{\bar{L}_z}$ and β_{V_z}.

For the scaling tests, the input parameters consist of three aspects: (1) the characteristic lengths $\bar{L}_x$, $\bar{L}_y$ and $\bar{L}_z$; (2) the material parameters ρ and σ_d (including the strain-rata-sensitivity and the strain hardening effects); (3) the external loadings such as the impulsive velocity V_z, the impact mass G with its impact velocity V_z, etc. When the geometric configuration in x-y plane is scaled by the factors $\beta_{\bar{L}_{xy}}$ ($\beta_{\bar{L}_{xy}} = \beta_{\bar{L}_x} = \beta_{\bar{L}_y}$), Eq. (29) will lead to the following three basic correction methods for the input parameters of scaled model, as follows:

(1) The impact velocity of scaled model can be corrected to $(V_z)_m^{cor} = (V_z)_p \beta_{V_z}^{cor}$ by the correction factor

$$\beta_{V_z}^{cor} = \left(\frac{\beta_{\bar{L}_z}}{\beta_{\bar{L}_{xy}}}\right) \sqrt{\frac{f_m\left\{\left(\varepsilon_{eq}\right)_p \left(\frac{\beta_{\bar{L}_z}}{\beta_{\bar{L}_{xy}}}\right)^2, \left(\dot{\varepsilon}_{eq}\right)_p \frac{\beta_{V_z}^{cor}}{\beta_{\bar{L}_z}} \left(\frac{\beta_{\bar{L}_z}}{\beta_{\bar{L}_{xy}}}\right)^2\right\}}{f_p\left\{\left(\varepsilon_{eq}\right)_p, \left(\dot{\varepsilon}_{eq}\right)_p\right\}} \frac{1}{\beta_\rho}}, \tag{30}$$

where the factors $\beta_{\bar{L}_{xy}}$, $\beta_{\bar{L}_z}$ and β_ρ are given according to the initial state of input parameters between the scaled model and the prototype. The superscript 'cor'

Preprints (www.preprints.org) | NOT PEER-REVIEWED | Posted: 26 February 2020 doi:10.20944/preprints202002.0394.v1

represents the correction for physical quantity.

(2) The thickness of scaled model can be corrected to $(\bar{L}_z)_m^{cor} = (L_z)_p \beta_{\bar{L}_z}^{cor}$ by the correction factor

$$\beta_{\bar{L}_z}^{cor} = \beta_{\bar{L}_{xy}} \beta_{V_z} \sqrt{\frac{f_p\left\{\left(\varepsilon_{eq}\right)_p, \left(\dot{\varepsilon}_{eq}\right)_p\right\}}{f_m\left\{\left(\varepsilon_{eq}\right)_p \left(\frac{\beta_{\bar{L}_z}^{cor}}{\beta_{\bar{L}_{xy}}}\right)^2, \left(\dot{\varepsilon}_{eq}\right)_p \frac{\beta_{V_z}}{\beta_{\bar{L}_z}^{cor}} \left(\frac{\beta_{\bar{L}_z}^{cor}}{\beta_{\bar{L}_{xy}}}\right)^2\right\}} \beta_\rho} \tag{31}$$

where the factors $\beta_{\bar{L}_{xy}}$, β_{V_z} and β_ρ are given according to the initial state of input parameters between the geometrically similar scaled model and the prototype.

(3) The density of scaled model can be corrected to $\rho_m^{cor} = \rho_p \beta_\rho^{cor}$ by the correction factor

$$\beta_\rho^{cor} = \frac{f_m\left\{\left(\varepsilon_{eq}\right)_p \left(\frac{\beta_{\bar{L}_z}}{\beta_{\bar{L}_{xy}}}\right)^2, \left(\dot{\varepsilon}_{eq}\right)_p \frac{\beta_{V_z}}{\beta_{\bar{L}_z}} \left(\frac{\beta_{\bar{L}_z}}{\beta_{\bar{L}_{xy}}}\right)^2\right\}}{f_p\left\{\left(\varepsilon_{eq}\right)_p, \left(\dot{\varepsilon}_{eq}\right)_p\right\}} \frac{1}{\beta_{V_z}^2} \left(\frac{\beta_{\bar{L}_z}}{\beta_{\bar{L}_{xy}}}\right)^2, \tag{32}$$

where the factors $\beta_{\bar{L}_{xy}}$, $\beta_{\bar{L}_z}$ and β_{V_z} are given according to the initial state of input parameters between the scaled model and the prototype. Therefore, the structural mass and the impact mass of scaled model are correspondingly corrected to $M_m^{cor} = M_p \beta_\rho^{cor} \left(\beta_{\bar{L}_x} \beta_{\bar{L}_y} \beta_{\bar{L}_z}\right)$ and $G_m^{cor} = G_p \beta_\rho^{cor} \left(\beta_{\bar{L}_x} \beta_{\bar{L}_y} \beta_{\bar{L}_z}\right)$, respectively. The correction for structural mass can be realized by using the technique of Jiang et al. (2016) in which the additional mass $\Delta M = (M)_p \left(\beta_\rho^{cor} - 1\right)$ is evenly and discreetly distributed into each components of the scaled model.

The solving method for $\beta_{V_z}^{cor}$ in Eq. (30) can use a simple fixed-point iterative scheme about $\beta_{V_z}^{cor}$ when $\left(\varepsilon_{eq}\right)_p$ and $\left(\dot{\varepsilon}_{eq}\right)_p$ are known. The solving method for $\beta_{\bar{L}_z}^{cor}$ in Eq. (31) and the solving method for β_ρ^{cor} in Eq. (32) are the same.

Preprints (www.preprints.org) | NOT PEER-REVIEWED | Posted: 26 February 2020 doi:10.20944/preprints202002.0394.v1

In addition, the combination of three basic correcting methods provides a comprehensive correction method for input parameters. When three correction factors $\beta_{V_z}^{cor}$, $\beta_{\bar{L}_z}^{cor}$ and β_{ρ}^{cor} are simultaneously substituted into Eq. (29), two of them can be given arbitrarily in advance, and the other one can be obtained after solving the equation. This means that, for these three correction factors, two of them can be corrected arbitrarily form the initial states of input parameters, while the other can be corrected according to Eq. (29). This comprehensive correction method can also be expressed as a more concisely equation as

$$\Pi_{\sigma_{eq}} = \underbrace{\frac{\rho_m^{cor}\left(\left(V_z\right)_m^{cor}\right)^2}{\left(\sigma_{eq}\right)_m}\left[\frac{\left(\bar{L}_{xy}\right)_m}{\left(\bar{L}_z\right)_m^{cor}}\right]^2}_{For\ scaled\ model} = \underbrace{\frac{\rho_p\left(V_z\right)_p^2}{\left(\sigma_{eq}\right)_p}\left[\frac{\left(\bar{L}_{xy}\right)_p}{\left(\bar{L}_z\right)_p}\right]^2}_{For\ prototype}. \tag{33}$$

It can be seen that the correction for the impact velocity, the geometrical thickness and the density is equivalent to the correction for the dimensionless number of equivalent stress. The above analysis indicated that the number $\Pi_{\sigma_{eq}}$ is the dominant similarity condition that input parameters must be satisfied for structures subjected to impact loads.

Finally, from the above correction methods, the addressing ability for the non-scaling problems can be summarized as follows:

(1) The material distortion has been included in the above correction methods since using the different density and constitutive equation between scaled model and prototype. Although the previous works (such as VSG and DLV) has been studied in detail through correcting the impact velocity and the density (or structural mass and impact mass), Eq. (31) provides a new correction method —correcting the geometric

Preprints (www.preprints.org) | NOT PEER-REVIEWED | Posted: 26 February 2020 doi:10.20944/preprints202002.0394.v1

thickness of scaled model.

(2) The geometric distortion of thickness (i.e., $\beta_{\bar{L}_z} \neq \beta_{\bar{L}_{xy}}$) can be compensate by the correction for impact velocity or density of scaled model (Eq. (30) or (32)).

(3) The distortion of gravity can be compensated by the correction for geometrical thickness or density of scaled model (Eq. (31) or (32)). When the transverse gravity acceleration g_z is considered for the geometrically similar structure ($\beta_{\bar{L}_z} = \beta_{\bar{L}_{xy}}$), the impact velocity and geometric thickness must respect the relation $\beta_{V_z} = \sqrt{\beta_{g_z}\beta_{\bar{L}_z}} = \sqrt{\beta_{\bar{L}_z}}$ ($\beta_{g_z} = 1$ usually). If substituting $\beta_{V_z} = \sqrt{\beta_{\bar{L}_z}^{cor}}$ into Eq. (31) (or $\beta_{V_z} = \sqrt{\beta_{\bar{L}_z}}$ into Eq. (32)), the correction factor $\beta_{\bar{L}_z}^{cor}$ (or β_{ρ}^{cor}) can be obtained to compensate the distortion caused by gravity effects.

(4) The more non-scaling problems can also be compensated by the combination of three basic correction methods. For example, when the geometric distortion of thickness ($\beta_{\bar{L}_z} \neq \beta_{\bar{L}_{xy}}$) and the transverse gravity acceleration g_z are considered at the same time, the impact velocity of scaled model can be corrected as $(V_z)_m^{cor} = (V_z)_p\beta_{V_z}^{cor} = (V_z)_p\sqrt{\beta_{\bar{L}_z}}$ by the first correction factor $\beta_{V_z}^{cor} = \sqrt{\beta_{\bar{L}_z}}$. Then, the substation of $\beta_{\bar{L}_z}$ and $\beta_{V_z}^{cor}$ into Eq. (33) can obtain the second correction factor β_{ρ}^{cor} to correct density of scaled model as $\rho_m^{cor} = \rho_p\beta_{\rho}^{cor}$. The combination of two correction factors can compensate the distortion caused by both gravity and geometric thickness.

The above analysis lays the foundation for the addressing ability of the non-scaling problems. These correction methods can be used in combination to compensate different distortion problems such as geometry, material and gravity distortion.

Preprints (www.preprints.org) | NOT PEER-REVIEWED | Posted: 26 February 2020 doi:10.20944/preprints202002.0394.v1

2.6. Transformation into cylindrical coordinate system

For the thin-plate problem, the derivations for similarity laws in above sections base on the cartesian coordinate system (x, y, z). When using the cylindrical coordinate system (r, θ, z), it is also very convenient.

In the cylindrical coordinate system (r, θ, z), the subscripts r, θ, z for physical quantity represent the r-axis direction, the θ-axis direction and the z-axis direction, respectively; the notations $\mathbb{R}$ and $\mathbb{A}$ represent the dimension of radius and angle, respectively; and $\bar{R}$ and $\bar{\theta}$ represent characteristic radius and characteristic angle, respectively. Then, three oriented dimensions of length in the cylindrical coordinate system are $\mathbb{L}_r = \mathbb{R}_r$, $\mathbb{L}_\theta = \mathbb{R}_r\mathbb{A}_\theta$ and $\mathbb{L}_z$, which similar to $\mathbb{L}_x$, $\mathbb{L}_y$ and $\mathbb{L}_z$; three oriented characteristic lengths in the cylindrical coordinate system are $\bar{L}_r = \bar{R}$, $\bar{L}_\theta = \bar{R}\bar{\theta}$ and $\bar{L}_z$, which similar to $\bar{L}_x$, $\bar{L}_y$ and $\bar{L}_z$; and three subscripts in the cylindrical coordinate system are r, θ and z, which similar to the subscripts x, y and z of cartesian coordinate system. The transformation for dimensions, characteristic lengths and subscripts from the cartesian coordinate system to the cylindrical coordinate system are summarized as follows:

$$\left.\begin{array}{ll} \textit{Dimension}: & \mathbb{L}_x \to \mathbb{L}_r = \mathbb{R}_r, \mathbb{L}_y \to \mathbb{L}_\theta = \mathbb{R}_r\mathbb{A}_\theta, \mathbb{L}_z \to \mathbb{L}_z \\ \textit{Characteristic length}: & \bar{L}_x \to \bar{L}_r, \bar{L}_y \to \bar{L}_\theta = \bar{L}_r\bar{\theta}, \bar{L}_z \to \bar{L}_z \\ \textit{Subscript}: & x \to r, y \to \theta, z \to z \end{array}\right\} \quad (34)$$

The dimensionless number of physical quantities in cylindrical coordinate system can be directly obtained. For example, the number $\Pi_{\sigma_r} = \frac{\rho V_z^2}{\sigma_r}\left(\frac{\bar{R}}{\bar{L}_z}\right)^2$ for σ_r being obtained from the expression $\Pi_{\sigma_x} = \frac{\rho V_z^2}{\sigma_x}\left(\frac{\bar{L}_x}{\bar{L}_z}\right)^2$; the number $\Pi_{\sigma_\theta} = \frac{\rho V_z^2}{\sigma_\theta}\left(\frac{\bar{R}\bar{\theta}}{\bar{L}_z}\right)^2$ for σ_θ

Preprints (www.preprints.org) | NOT PEER-REVIEWED | Posted: 26 February 2020 doi:10.20944/preprints202002.0394.v1

being obtained from the expression $\Pi_{\sigma_y} = \frac{\rho V_z^2}{\sigma_y}\left(\frac{\bar{L}_y}{\bar{L}_z}\right)^2$; the number $\Pi_G = \frac{G}{\rho \bar{R}^2 \bar{\theta} \bar{L}_z}$ for G being obtained from the expression $\Pi_G = \frac{G}{\rho \bar{L}_x \bar{L}_y \bar{L}_z}$; the number $\Pi_{\sigma_{eq}} = \frac{\rho V_z^2}{\sigma_{eq}}\left(\frac{\bar{R}}{\bar{L}_z}\right)^2$ for σ_{eq} being obtained from the expression $\Pi_{\sigma_{eq}} = \frac{\rho V_z^2}{\sigma_{eq}}\left(\frac{\bar{L}_{xy}}{\bar{L}_z}\right)^2$.

The scaling factors of physical quantities in cylindrical coordinate system can also be obtained easily from their expression in cartesian coordinate system. For example, the factor $\beta_{\sigma_r} = \left(\beta_\rho \beta_{V_z}^2\right)\left(\beta_{\bar{R}}/\beta_{\bar{L}_z}\right)^2$ for σ_r being obtained from the expression $\beta_{\sigma_x} = \left(\beta_\rho \beta_{V_z}^2\right)\left(\beta_{\bar{L}_x}/\beta_{\bar{L}_z}\right)^2$; the factor $\beta_{\sigma_\theta} = \left(\beta_\rho \beta_{V_z}^2\right)\left(\beta_{\bar{R}} \beta_{\bar{\theta}}/\beta_{\bar{L}_z}\right)^2$ for σ_θ being obtained from the expression $\beta_{\sigma_y} = \left(\beta_\rho \beta_{V_z}^2\right)\left(\beta_{\bar{L}_y}/\beta_{\bar{L}_z}\right)^2$; the factor $\beta_G = \beta_\rho\left(\beta_{\bar{R}}^2 \beta_{\bar{\theta}} \beta_{\bar{L}_z}\right)$ for G being obtained from the expression $\beta_G = \beta_\rho\left(\beta_{\bar{L}_x} \beta_{\bar{L}_y} \beta_{\bar{L}_z}\right)$; the factor $\beta_{\sigma_{eq}} = \left(\beta_\rho \beta_{V_z}^2\right)\left(\beta_{\bar{R}}/\beta_{\bar{L}_z}\right)^2$ for σ_{eq} being obtained from the expression $\beta_{\sigma_{eq}} = \left(\beta_\rho \beta_{V_z}^2\right)\left(\beta_{\bar{L}_{xy}}/\beta_{\bar{L}_z}\right)^2$.

3. Analytical verification

In this section, three analytical models for beam, plate and shell are used to verify the effectiveness of the ODLV numbers for the geometric and material distortion.

3.1. The beams subjected to impact mass and impulsive velocity

The impact models of beams subjected to impact mass or impulsive velocity are studied as shown in Fig. 2. The beams are made of the rigid-plastic materials. For the clamped beams (Fig. 2b and c), the effects of finite displacements are taken into account.

Preprints (www.preprints.org) | NOT PEER-REVIEWED | Posted: 26 February 2020 doi:10.20944/preprints202002.0394.v1

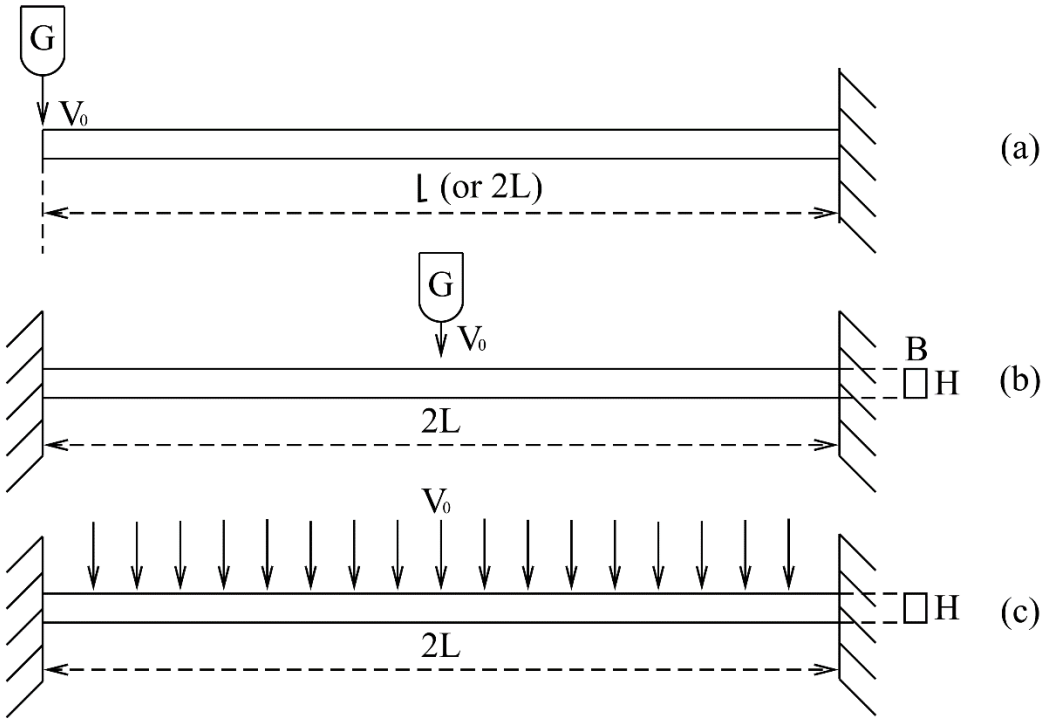

Fig. 2 Beams subjected to impact loading. (a) a cantilever subjected to mass impact at the free end; (b) a clamped beam subjected to impulsive velocity on entire span; (c) a clamped beam subjected to impact mass at mid span.

3.1.1. Response equations

For a cantilever subjected to mass impact (Parkes, 1955; Yu and Qiu, 2018), as shown in Fig. 2a, the maximum permanent transverse displacement (W_f) at the mid-span is given as

$$W_f = \frac{\mu V_0^2 l^2 \gamma^2}{3\Psi_0}\left[\frac{1}{1+2\kappa} + 2\ln\left(1+\frac{1}{2\kappa}\right)\right], \tag{35}$$

where μ is the mass per unit length; and $\kappa = G/\mu l$ is the mass ratio of impact mass to structure mass.

The final rotation angle (α_f) at the root is given as

$$\alpha_f = \frac{\mu l V_0^2}{6\Psi_0}(1+3\kappa)\left(1+\frac{1}{2\kappa}\right)^{-2}. \tag{36}$$

Preprints (www.preprints.org) | NOT PEER-REVIEWED | Posted: 26 February 2020 doi:10.20944/preprints202002.0394.v1

The final response time (T_f) is given as

$$T_f = \frac{GV_0 l}{\Psi_0}. \tag{37}$$

For clamped beam subjected to impact mass (Fig. 2b), the maximum permanent transverse displacement (W_f) at the mid-span is given as (Liu and Jones, 1988)

$$\frac{W_f}{H} = \frac{1}{2}\left[\left(1+\frac{2GV_0^2 L}{BH^3\sigma_d}\right)^{1/2} - 1\right]. \tag{38}$$

The equivalent strain is given as (Alves and Jones, 2002)

$$\varepsilon_{eq} = \begin{cases} \sqrt{\left(3\frac{W_f H}{L^2}\right)^2 + \left(\frac{4c}{\sqrt{3}}\frac{W_f}{L}\right)^2}, & for\ \frac{W_f}{H} \le 1 \\ \sqrt{\left\{\frac{1}{2}\left(\frac{H}{L}\right)^2\left[\left(\frac{W_f}{H}\right)^2 + 5\right]\right\}^2 + \left(\frac{4c}{\sqrt{3}}\frac{W_f}{L}\right)^2}, & for\ \frac{W_f}{H} > 1 \end{cases}, \tag{39}$$

where c is dimensional constant. The first term in radical sign of the right-hand side introduces the membrane strain and the bending strain. The second term introduces the transverse shear strain $\gamma_{xz} = 4cW_f/L$.

For clamped beam subjected to impulsive velocity (Fig. 2c), the maximum permanent transverse displacement (W_f) at the mid-span is given as (Jones, 1989)

$$\frac{W_f}{H} = \frac{1}{2}\left[\left(1+\frac{3\rho V_0^2 L^2}{\sigma_d H^2}\right)^{1/2} - 1\right]. \tag{40}$$

And the average strain rate ($\dot{\varepsilon}_{ave}$) is considered as (Jones, 1989)

$$\dot{\varepsilon}_{ave} = \frac{V_0 W_f}{3\sqrt{2}L^2}. \tag{41}$$

3.1.2. Dimensionless expression

For cantilever considering rectangular cross-section (i.e., $\Psi_0 = \sigma_d BH^2/4$; $\mu =$

Preprints (www.preprints.org) | NOT PEER-REVIEWED | Posted: 26 February 2020 doi:10.20944/preprints202002.0394.v1

ρBH), Eqs. (35)-(37) can be changed into the following forms

$$\frac{W_f}{H}=\frac{16}{3}\frac{\rho V_0^2}{\sigma_d}\left(\frac{L}{H}\right)^2\kappa^2\left[\frac{1}{1+2\kappa}+2\ln\left(1+\frac{1}{2\kappa}\right)\right], \tag{42}$$

$$\alpha_f\left(\frac{H}{L}\right)=\frac{16}{3}\frac{\rho V_0^2}{\sigma_d}\left(\frac{L}{H}\right)^2(1+3\kappa)\left(1+\frac{1}{2\kappa}\right)^{-2} \tag{43}$$

and

$$\frac{T_f V_0}{H}=16\frac{\rho V_0^2}{\sigma_d}\left(\frac{L}{H}\right)^2\kappa, \tag{44}$$

respectively.

Similarly, for clamped beam subjected to impact mass, Eq. (38) can be changed into the following form

$$\frac{W_f}{H}=\frac{1}{2}\left[\left(1+2\frac{\rho V_0^2}{\sigma_{\mathrm{d}}}\left(\frac{L}{H}\right)^2\frac{G}{\rho LBH}\right)^{1/2}-1\right]. \tag{45}$$

If the shear strain is neglected, Eq. (39) can be changed into the following form

$$\begin{aligned}\varepsilon_{eq}\left(\frac{L}{H}\right)^2&=\begin{cases}3\dfrac{W_f}{H}, & for\ \dfrac{W_f}{H}\le 1\\ \dfrac{1}{2}\left[\left(\dfrac{W_f}{H}\right)^2+5\right], & for\ \dfrac{W_f}{H}>1\end{cases}\\ &=\begin{cases}\dfrac{3}{2}\left[\left(1+2\dfrac{\rho V_0^2}{\sigma_{\mathrm{d}}}\left(\dfrac{L}{H}\right)^2\dfrac{G}{\rho LBH}\right)^{1/2}-1\right], & for\ \dfrac{W_f}{H}\le 1\\ \dfrac{1}{8}\left[\left(1+2\dfrac{\rho V_0^2}{\sigma_{\mathrm{d}}}\left(\dfrac{L}{H}\right)^2\dfrac{G}{\rho LBH}\right)^{1/2}-1\right]^2+\dfrac{5}{2}, & for\ \dfrac{W_f}{H}>1\end{cases}\end{aligned} \tag{46}$$

For clamped beam subjected to impulsive velocity, Eq. (40) can be changed into the following form

Preprints (www.preprints.org) | NOT PEER-REVIEWED | Posted: 26 February 2020 doi:10.20944/preprints202002.0394.v1

$$\frac{W_f}{H}=\frac{1}{2}\left[\left(1+3\frac{\rho V_0^2}{\sigma_{\mathrm{d}}}\left(\frac{L}{H}\right)^2\right)^{1/2}-1\right]. \tag{47}$$

The substitution of Eq. (47) into Eq. (41) will lead to the following form

$$\frac{\dot{\varepsilon}_{ave}H}{V_0}\left(\frac{L}{H}\right)^2=\frac{1}{3\sqrt{2}}\frac{W_f}{H}=\frac{1}{6\sqrt{2}}\left[\left(1+3\frac{\rho V_0^2}{\sigma_{\mathrm{d}}}\left(\frac{L}{H}\right)^2\right)^{1/2}-1\right]. \tag{48}$$

Equations (42)-(48) show that the number $\frac{W_f}{H}$, the number $\frac{\rho V_0^2}{\sigma_d}\left(\frac{L}{H}\right)^2$, the number $\frac{G}{\rho LBH}$ (only for mass impact), the number $\alpha_f\left(\frac{H}{L}\right)$, the number $\frac{T_f V_0}{H}$, the number $\varepsilon_{eq}\left(\frac{L}{H}\right)^2$ and the number $\frac{\dot{\varepsilon}_{ave}H}{V_0}\left(\frac{L}{H}\right)^2$ are seven independent dimensionless numbers in impact models of beams, which is in full accord with the number Π_{δ_z}, the number $\Pi_{\sigma_{eq}}$, the number Π_G, the number $\frac{\Pi_{\delta_z}}{\Pi_{\delta_x}}=\left[\frac{\delta_z}{\bar{L}_z}\right]/\left[\frac{\delta_x}{\bar{L}_x}\left(\frac{\bar{L}_x}{\bar{L}_z}\right)^2\right]=\left[\frac{\delta_z}{\delta_x}\left(\frac{\bar{L}_z}{\bar{L}_x}\right)\right]=\left[\alpha_{xz}\left(\frac{\bar{L}_z}{\bar{L}_x}\right)\right]=\Pi_{\alpha_{xz}}$, the number Π_t, the number $\Pi_{\varepsilon_{eq}}$ and the number $\Pi_{\dot{\varepsilon}_{eq}}$ in the ODLV system, respectively. In addition, for shear strain $\gamma_{xz}=4cW_f/L$ of Eq. (39), the new expression $\gamma_{xz}\frac{L}{H}=4c\frac{W_f}{H}$ indicates the number $\gamma_{xz}\left(\frac{L}{H}\right)$ is also an important dimensionless numbers, which is in full accord with the number $\Pi_{\gamma_{xz}}$ in the ODLV system.

For the previous scalar DLV system, Eq. (38) would be expressed to the form $\frac{W_f}{L}=\frac{1}{2}\frac{H}{L}\left\{\left[1+2\left(\frac{\rho V_0^2}{\sigma_d}\left(\frac{L}{H}\right)^2\right)\left(\frac{G}{\rho L^3}\frac{L}{B}\frac{L}{H}\right)\right]^{1/2}-1\right\}$ by five DLV numbers $\frac{W_f}{L}$, $\frac{L}{H}$, $\frac{L}{B}$, $\frac{\rho V_0^2}{\sigma_d}$ and $\frac{G}{\rho L^3}$. After considering the direction of physical quantity, these five DLV numbers are naturally grouped as three ODLV numbers $\frac{W_f}{H}$, $\frac{\rho V_0^2}{\sigma_d}\left(\frac{L}{H}\right)^2$ and $\frac{G}{\rho LBH}$, as shown in Eq. (45). It is evident that, compared with the DLV system, the ODLV system have ideal and perfect ability to express the dimensionless response equations of structural impact.

Preprints (www.preprints.org) | NOT PEER-REVIEWED | Posted: 26 February 2020 doi:10.20944/preprints202002.0394.v1

3.1.3. Scaling analysis

For the scaled model and the prototype, Eq. (42) can be written as

$$\frac{\left(W_f\right)_{\mathrm{m}}}{H_{\mathrm{m}}}=\frac{16}{3}\frac{\rho_{\mathrm{m}}\left(V_0\right)_m^2}{\left(\sigma_d\right)_{\mathrm{m}}}\left(\frac{L_{\mathrm{m}}}{H_{\mathrm{m}}}\right)^2\kappa_m^2\left[\frac{1}{1+2\kappa_{\mathrm{m}}}+2\ln\left(1+\frac{1}{2\kappa_{\mathrm{m}}}\right)\right] \tag{49}$$

and

$$\frac{\left(W_f\right)_p}{H_p}=\frac{16}{3}\frac{\rho_p\left(V_0\right)_p^2}{\left(\sigma_d\right)_p}\left(\frac{L_p}{H_p}\right)^2\kappa_p^2\left[\frac{1}{1+2\kappa_p}+2\ln\left(1+\frac{1}{2\kappa_p}\right)\right], \tag{50}$$

respectively.

The similarity between the scaled model and the prototype means Eq. (49) and Eq. (50) are the same, which leads to three scaling relations as

$$\left.\begin{aligned}\frac{\left(W_f\right)_{\mathrm{m}}}{H_{\mathrm{m}}}&=\frac{\left(W_f\right)_p}{H_p}\\ \frac{\rho_{\mathrm{m}}\left(V_0\right)_m^2}{\left(\sigma_d\right)_{\mathrm{m}}}\left(\frac{L_{\mathrm{m}}}{H_{\mathrm{m}}}\right)^2&=\frac{\rho_p\left(V_0\right)_p^2}{\left(\sigma_d\right)_p}\left(\frac{L_p}{H_p}\right)^2\\ \kappa_{\mathrm{m}}=\frac{G_m}{\rho_m\left(2L_m\right)B_mH_m}&=\kappa_p=\frac{G_p}{\rho_p\left(2L_p\right)B_pH_p}\end{aligned}\right\} \tag{51a-c}$$

Equation. (51a-c) can be rewritten as three scaling relations $\beta_{W_f}=\beta_H$, $\beta_{\sigma_d}=\left(\beta_\rho\beta_{V_0}^2\right)(\beta_L/\beta_H)^2$ and $\beta_G=\beta_\rho(\beta_L\beta_B\beta_H)$. In the same way, Eqs. (43)-(48) can obtain other four scaling relations $\left(\alpha_f\right)_m\left(\frac{Hm}{Lm}\right)=\left(\alpha_f\right)_p\left(\frac{Hp}{Lp}\right)$, $\frac{\left(T_f\right)_m(V_0)_m}{Hm}=\frac{\left(T_f\right)_p(V_0)_p}{Hp}$, $\left(\varepsilon_{eq}\right)_m\left(\frac{Lm}{Hm}\right)^2=\left(\varepsilon_{eq}\right)_p\left(\frac{Lp}{Hp}\right)^2$ and $\frac{(\dot{\varepsilon}_{ave})_mHm}{(V_0)_m}\left(\frac{Lm}{Hm}\right)^2=\frac{(\dot{\varepsilon}_{ave})_pHp}{(V_0)_p}\left(\frac{Lp}{Hp}\right)^2$ (or $\beta_{\alpha_f}=(\beta_L/\beta_H)$, $\beta_{T_f}=\beta_H/\beta_{V_0}$, $\beta_{\varepsilon_{eq}}=(\beta_H/\beta_L)^2$ and $\beta_{\dot{\varepsilon}_{ave}}=\left(\beta_{V_0}/\beta_H\right)(\beta_H/\beta_L)^2$).

Based on the above scaling relations, the scaling testing for three beams could be implemented by correcting the impact velocity, the geometrical thickness or the density, as follows:

Preprints (www.preprints.org) | NOT PEER-REVIEWED | Posted: 26 February 2020 doi:10.20944/preprints202002.0394.v1

- Correction for the impact velocity: if the input parameters satisfy the relations $\beta_\rho = \rho_m/\rho_p$, $\beta_L = L_m/L_p$, $\beta_B = B_m/B_p$, $\beta_H = H_m/H_p$, $\beta_G = \beta_\rho(\beta_L\beta_B\beta_H)$ and $\beta_{V_0}^{cor} = (\beta_H/\beta_L)\sqrt{\beta_{\sigma_d}/\beta_\rho}$, the output parameters will satisfy the relations $\beta_{W_f} = \beta_H$, $\beta_{\alpha_f} = (\beta_L/\beta_H)$, $\beta_{T_f} = \beta_H/\beta_{V_0}^{cor}$, $\beta_{\varepsilon_{eq}} = (\beta_H/\beta_L)^2$ and $\beta_{\dot{\varepsilon}_{ave}} = \left(\beta_{V_0}^{cor}/\beta_H\right)(\beta_H/\beta_L)^2$.
- Correction for the geometrical thickness: if the input parameters satisfy the relations $\beta_\rho = \rho_m/\rho_p$, $\beta_L = L_m/L_p$, $\beta_B = B_m/B_p$, $\beta_{V_0} = (V_0)_m/(V_0)_p$, $\beta_H^{cor} = \beta_L\beta_{V_0}\sqrt{\beta_\rho/\beta_{\sigma_d}}$ and $\beta_G = \beta_\rho(\beta_L\beta_B\beta_H^{cor})$, the output parameters will satisfy the relations $\beta_{W_f} = \beta_H^{cor}$, $\beta_{\alpha_f} = (\beta_L/\beta_H^{cor})$, $\beta_{T_f} = \beta_H^{cor}/\beta_{V_0}$, $\beta_{\varepsilon_{eq}} = (\beta_H^{cor}/\beta_L)^2$ and $\beta_{\dot{\varepsilon}_{ave}} = \left(\beta_{V_0}/\beta_H^{cor}\right)(\beta_H^{cor}/\beta_L)^2$.
- Correction for the density: if the input parameters satisfy the relations $\beta_L = L_m/L_p$, $\beta_B = B_m/B_p$, $\beta_H = H_m/H_p$, $\beta_{V_0} = (V_0)_m/(V_0)_p$, $\beta_\rho^{cor} = (\beta_H/\beta_L)^2\left(\beta_{\sigma_d}/\beta_{V_0}^2\right)$ and $\beta_G = \beta_\rho^{cor}(\beta_L\beta_B\beta_H)$, the output parameters will satisfy the relations $\beta_{W_f} = \beta_H$, $\beta_{\alpha_f} = (\beta_L/\beta_H)$, $\beta_{T_f} = \beta_H/\beta_{V_0}$, $\beta_{\varepsilon_{eq}} = (\beta_H/\beta_L)^2$ and $\beta_{\dot{\varepsilon}_{ave}} = \left(\beta_{V_0}/\beta_H\right)(\beta_H/\beta_L)^2$.

The scaling procedures can also be expressed by the dimensionless numbers. For example, the correction procedure of the impact velocity can be re-expressed as: if the input parameters satisfy $\frac{\rho_m[(V_0)_m^{cor}]^2}{(\sigma_d)_m}\left(\frac{L_m}{H_m}\right)^2 = \frac{\rho_p(V_0)_p^2}{(\sigma_d)_p}\left(\frac{L_p}{H_p}\right)^2$ and $\frac{G_m}{\rho_m L_m B_m H_m} = \frac{G_p}{\rho_p L_p B_p H_p}$, the output parameters will satisfy $\frac{(W_f)_m}{H_m} = \frac{(W_f)_p}{H_p}$, $\frac{(\alpha_f)_m H_m}{L_m} = \frac{(\alpha_f)_p H_p}{L_p}$, $\frac{(T_f)_m(V_0)_m^{cor}}{H_m} = \frac{(T_f)_p(V_0)_p}{H_p}$, $(\varepsilon_{eq})_m\left(\frac{L_m}{H_m}\right)^2 = (\varepsilon_{eq})_p\left(\frac{L_p}{H_p}\right)^2$ and $\frac{(\dot{\varepsilon}_{ave})_m H_m}{(V_0)_m^{cor}}\left(\frac{L_m}{H_m}\right)^2 = \frac{(\dot{\varepsilon}_{ave})_p H_p}{(V_0)_p}\left(\frac{L_p}{H_p}\right)^2$. Obviously, these two expression procedures are equivalent. In addition, for the strain-rate-sensitivity and strain hardening materials, $\beta_{V_0}^{cor}$, β_H^{cor} and β_ρ^{cor}

Preprints (www.preprints.org) | NOT PEER-REVIEWED | Posted: 26 February 2020 doi:10.20944/preprints202002.0394.v1

can be solved by Eq. (30), Eq. (31) and Eq. (32), respectively.

The three basic scaling procedures actually include the non-scaling problems of the geometric distortion (i.e., at least two of three factors β_L, β_B and β_H are not equal) and the distortion of different materials (i.e., $\beta_\rho \neq 1$ or $\beta_{\sigma_d} \neq 1$).

It can be learned from the analysis of beams that the scaling relations of structural impact can be obtained directly by the use of the ODLV numbers. When we conduct a scaling test, the dimensionless numbers of input parameters determine the sufficient conditions of similarity, while the dimensionless numbers of output parameters determine the mapping relationship of structural response between scaled model and prototype. In this procedure, the ODLV bases provide five essential scaling factors, i.e. the density factor β_ρ, three geometric factors $\beta_{\bar{L}_x}$, $\beta_{\bar{L}_y}$ and $\beta_{\bar{L}_z}$ and the velocity factor β_{V_z}. When the geometric configuration in the x and y directions is scaled by the factors $\beta_{\bar{L}_x}$ and $\beta_{\bar{L}_y}$, the velocity factor β_{V_z}, the geometric thickness factor $\beta_{\bar{L}_z}$ and the density factor β_ρ can be corrected to address the non-scaling problems.

3.2. The rectangular plates subjected to impact mass and impulsive velocity

The impact models of a simple or clamp supported rectangular plates subjected to impact mass or impulsive velocity are studied as shown in Fig. 3. The plates are made of the rigid-plastic materials and already take into account the effects of the finite displacements.

Preprints (www.preprints.org) | NOT PEER-REVIEWED | Posted: 26 February 2020 doi:10.20944/preprints202002.0394.v1

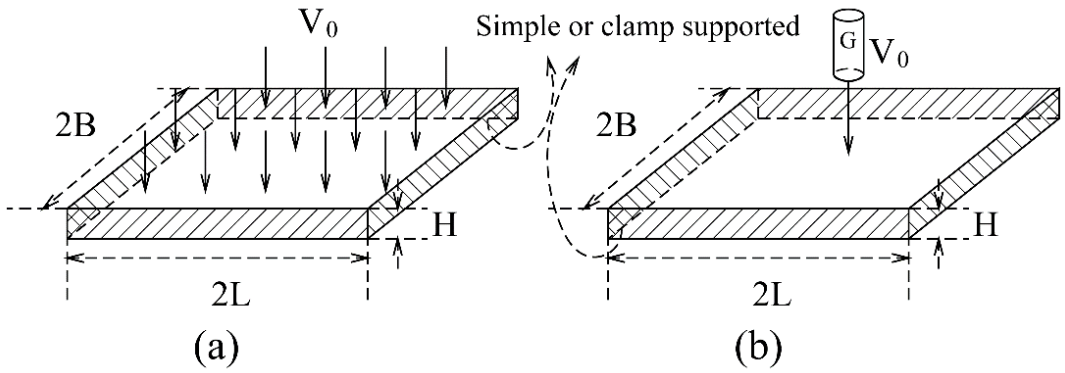

Fig. 3 A simple or clamp supported rectangular plate subjected to (a) impulsive velocity or (b) impact mass.

3.2.1. Response equations

For impulsive velocity loading, the maximum permanent transverse displacement (W_f) for simple supports and clamped supports are given as (Jones, 1989)

$$\frac{W_f}{H}=\frac{(3-\xi_0)\left\{\left[1+\frac{2}{3}\lambda\xi_0^2\left(1-\xi_0+\frac{1}{2-\xi_0}\right)\right]^{1/2}-1\right\}}{4\left[1+(\xi_0-1)(\xi_0-2)\right]} \tag{52}$$

and

$$\frac{W_f}{H}=\frac{(3-\xi_0)\left\{\left[1+\frac{1}{6}\lambda\xi_0^2\left(1-\xi_0+\frac{1}{2-\xi_0}\right)\right]^{1/2}-1\right\}}{2\left[1+(\xi_0-1)(\xi_0-2)\right]}, \tag{53}$$

respectively, where $\lambda=\frac{\mu' V_0^2 L^2}{(\sigma_d H^2/4)H}$, $\xi_0=\zeta\left[(3+\zeta^2)^{1/2}-\zeta\right]$, $\zeta=\frac{B}{L}$; and $\mu'=\rho H$ is mass per unit surface area.

For impact mass loading, the maximum permanent transverse displacement (W_f) for simple and clamped supports is given as (Jones, 2012)

$$\frac{W_f}{H}=\frac{(1+\omega)}{2}\left[\sqrt{1+\frac{12\zeta\Omega\kappa(1+6\kappa)}{(1+\zeta^2)(1+\omega)^2(1+3\kappa)^2}}-1\right] \tag{54}$$

Preprints (www.preprints.org) | NOT PEER-REVIEWED | Posted: 26 February 2020 doi:10.20944/preprints202002.0394.v1

where $\Omega = \frac{GV_0^2}{4\sigma_d H^3}$; $\kappa = G/[\mu'(2L)(2B)]$ is mass ratios; and ω is dimensionless moment resistance at supports (n'=0 and 1 for simply and fully clamped supports, respectively).

3.2.2. Dimensionless expression and scaling analysis

It is obvious that Eq. (52) (or Eq. (53)) can be changed into the following form

$$\frac{W_f}{H} = f'\left\{\frac{\rho V_0^2}{\sigma_d}\left(\frac{L}{H}\right)^2, \zeta\right\}. \tag{55}$$

where f' is function relation about Eq. (52) (or Eq. (53)).

Similarly, Eq. (54) can be changed into the following form

$$\frac{W_f}{H} = \frac{(1+\omega)}{2}\left[\sqrt{1+\frac{\rho V_0^2}{\sigma_d}\left(\frac{L}{H}\right)^2 \frac{3\zeta^2\kappa^2(1+6\kappa)}{\left(1+\zeta^2\right)(1+\omega)^2(1+3\kappa)^2}} - 1\right]. \tag{56}$$

Equations (55)-(56) show that the number $\frac{W_f}{H}$, the number $\frac{\rho V_0^2}{\sigma_d}\left(\frac{L}{H}\right)^2$, the number $\frac{G}{\rho LBH}$ and the number $\frac{B}{L}$ are four independent dimensionless numbers for the impact models of plate, which are in full accord with the number Π_{δ_z}, the number $\Pi_{\sigma_{eq}}$, the number Π_G and the number Π_{x-y} (Sect. 2.3) in the ODLV system. In addition, the differences between Eqs. (55), (56) and Eqs. (42), (45), (47) show the number $\frac{B}{L}$ for plates does exist but not for beams in response equation. The main reason is that the plates are usually considered as two-dimensional structure while the beams are one-dimensional structure.

In addition, for scaling analysis, the numbers $\frac{W_f}{H}$, $\frac{\rho V_0^2}{\sigma_d}\left(\frac{L}{H}\right)^2$, $\frac{G}{\rho LBH}$ and $\frac{B}{L}$ require the input and output parameters between scaled model and prototype must satisfy four scaling relations $\frac{(W_f)_m}{H_m} = \frac{(W_f)_p}{H_p}$, $\frac{\rho_m (V_0)_m^2}{(\sigma_d)_m}\left(\frac{L_m}{H_m}\right)^2 = \frac{\rho_p (V_0)_p^2}{(\sigma_d)_p}\left(\frac{L_p}{H_p}\right)^2$, $\frac{G_m}{\rho_m L_m B_m H_m} =$

Preprints (www.preprints.org) | NOT PEER-REVIEWED | Posted: 26 February 2020 doi:10.20944/preprints202002.0394.v1

$\frac{G_p}{\rho_p L_p B_p H_p}$ and $\frac{B_m}{L_m} = \frac{B_p}{L_p}$ (or $\beta_{W_f} = \beta_H$, $\beta_{\sigma_d} = (\beta_\rho \beta_{V_0}^2)(\beta_L/\beta_H)^2$, $\beta_G = \beta_\rho(\beta_L \beta_B \beta_H)$ and $\beta_B = \beta_L$). Then, the scaling testing for the simple or clamp supported plates can be implemented as the scaling testing for beams of Sect. 3.1.3 in which the length and width in the x-y plane of plates are scaled equally by the number $\frac{B}{L}$.

It can be learned from the above analysis of beams and plates that, for structures subjected to impulsive velocity and impact mass, the response equations of final deformation, rotation angle, time, strain and strain rate all can be expressed as functions among the ODLV numbers. The independent variables of these functional relations are the dimensionless numbers of input parameters (i.e., the number $\Pi_{\sigma_{eq}}$ for equivalent stress (or dynamic flow stress), the number Π_G for impact mass and the number Π_{x-y} for the isotropic x-y plane, etc.), while the dependent variables are the dimensionless numbers of output parameters (i.e., the number Π_{δ_z} for deflections, the number $\Pi_{\alpha_{xz}}$ for rotation angle, the number Π_t for time, the number $\Pi_{\varepsilon_{eq}}$ for equivalent strain and the number $\Pi_{\dot{\varepsilon}_{eq}}$ for equivalent strain rate, etc.). It is also significant to find that the dimensionless response equation of final deflection has been verified by more impact models of beams, square and rectangular plates, circular plates and circular membranes (Zhao, 1998b; Hu, 2009).

3.3 A spherical shell subjected to impulsive velocity

The impact model of a spherical shell subjected to a spherically symmetric radially outwards impulsive velocity is studied as shown in Fig. 4. The shell is made of the rigid-plastic materials. The impact model is built in spherical coordinate system (r, α_a,

Preprints (www.preprints.org) | NOT PEER-REVIEWED | Posted: 26 February 2020 doi:10.20944/preprints202002.0394.v1

α_b).

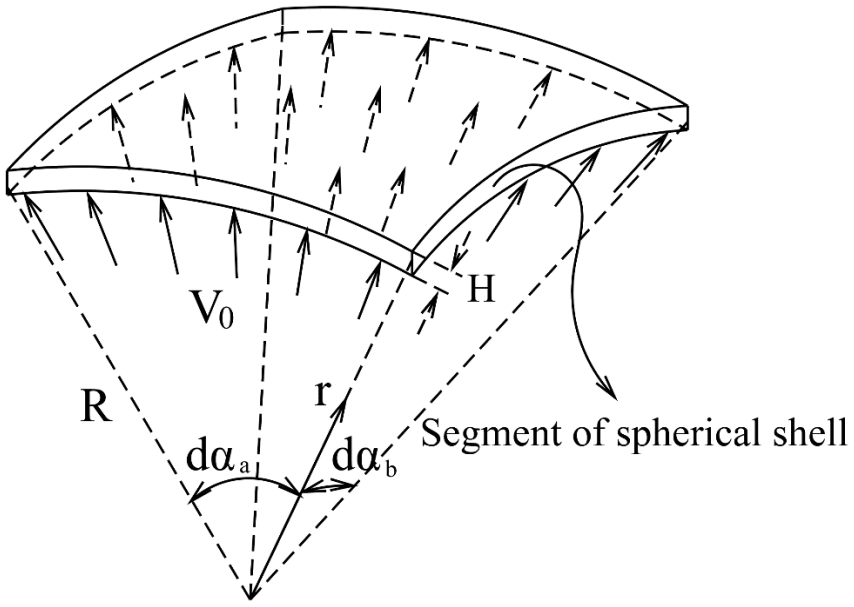

Fig. 4 Segment of spherical shell subjected to impulsive velocity.

3.3.1. Response equations

The maximum permanent radial displacement (W_f) is given as (Jones, 1989)

$$W_f = -\frac{\mu' R V_0^2}{4N_0'}. \tag{57}$$

where R is radius of the sphere; $\mu' = \rho H$ is mass per unit surface area of shell; and $N_0' = \sigma_d H$ is the fully plastic membrane force for the shell cross-section.

The final response time is given as

$$T_f = \frac{\mu' V_0 R}{2N_0'}. \tag{58}$$

The biaxial membrane strains in the spherical shell are $\varepsilon_{\alpha_a} = \varepsilon_{\alpha_b} = -W_f/R$. When substituting Eq. (57), the permanent membrane strain (ε_f) is derived as

$$\varepsilon_f = -\frac{W_f}{R} = -\frac{\mu' V_0^2}{4N_0'}. \tag{59}$$

3.3.2. Dimensionless expression and scaling analysis

Preprints (www.preprints.org) | NOT PEER-REVIEWED | Posted: 26 February 2020 doi:10.20944/preprints202002.0394.v1

Equations (57)-(59) can be changed into the following forms

$$\frac{W_f}{H} = -\frac{1}{4}\frac{\rho V_0^2}{\sigma_d}\left(\frac{R}{H}\right), \tag{60}$$

$$\frac{T_f V_0}{H} = \frac{1}{2}\frac{\rho V_0^2}{\sigma_d}\left(\frac{R}{H}\right) \tag{61}$$

and

$$\varepsilon_f\left(\frac{R}{H}\right) = \frac{1}{4}\frac{\rho V_0^2}{\sigma_d}\left(\frac{R}{H}\right), \tag{62}$$

respectively.

Equations (60)-(62) show that the number $\frac{W_f}{H}$, the number $\frac{\rho V_0^2}{\sigma_d}\left(\frac{R}{H}\right)$, the number $\frac{T_f V_0}{H}$ and the number $\varepsilon_f\left(\frac{R}{H}\right)$ are four independent dimensionless numbers for this impact model of spherical shell. Obviously, the numbers $\frac{W_f}{H}$ and $\frac{T_f V_0}{H}$ are in full accord with the ODLV numbers Π_{δ_z} and Π_t in the spherical coordinate system, respectively; the number $\frac{\rho V_0^2}{\sigma_d}\left(\frac{R}{H}\right)$ can be obtained by reducing the exponent of $\left(\frac{\bar{R}}{\bar{L}_z}\right)$ from the ODLV number $\Pi_{\sigma_{eq}} = \frac{\rho V_z^2}{\sigma_{eq}}\left(\frac{\bar{R}}{\bar{L}_z}\right)^2$ in the spherical coordinate system; the number $\varepsilon_f\left(\frac{R}{H}\right)$ can be obtained by reducing the exponent of $\left(\frac{\bar{R}}{\bar{L}_z}\right)$ from the ODLV number $\Pi_{\varepsilon_{eq}} = \varepsilon_{eq}\left(\frac{\bar{R}}{\bar{L}_z}\right)^2$ in the spherical coordinate system. In this case of shell, the impulsive velocity V_0 is radial and the characteristic lengths of spherical surface is $\bar{L}_{\alpha_a} = \bar{L}_{\alpha_b} = \pi R$ where π is circumference ratio. It is also significant to find that, for the final deflection response of the cylindrical shells subjected to uniform impulsive velocity, the functional relations between the number $\frac{W_f}{H}$ and the number $\frac{\rho V_0^2}{\sigma_d}\left(\frac{R}{H}\right)$ has been verified by equation analysis in the work of Shi and Gao (2001). The power exponent of characteristic length for the shell is different from that of the plate, which could be mainly caused by the initial curvature of the shell.

Preprints (www.preprints.org) | NOT PEER-REVIEWED | Posted: 26 February 2020 doi:10.20944/preprints202002.0394.v1

For scaling analysis, the numbers $\frac{W_f}{H}$, $\frac{\rho V_0^2}{\sigma_d}\left(\frac{R}{H}\right)$, $\frac{T_f V_0}{H}$ and $\varepsilon_f\left(\frac{R}{H}\right)$ require the input and output parameters between scaled model and prototype must satisfy four scaling relations $\frac{(W_f)_m}{H_m} = \frac{(W_f)_p}{H_p}$, $\frac{\rho_m (V_0)_m^2}{(\sigma_d)_m}\left(\frac{R_m}{H_m}\right) = \frac{\rho_p (V_0)_p^2}{(\sigma_d)_p}\left(\frac{R_p}{H_p}\right)$, $\frac{(T_f)_m (V_0)_m}{H_m} = \frac{(T_f)_p (V_0)_p}{H_p}$ and $(\varepsilon_f)_m\left(\frac{R_m}{H_m}\right) = (\varepsilon_f)_p\left(\frac{R_p}{H_p}\right)$ (or $\beta_{W_f} = \beta_H$, $\beta_{\sigma_d} = (\beta_\rho \beta_{V_0}^2)(\beta_R/\beta_H)$, $\beta_{T_f} = \beta_H/\beta_{V_0}$ and $\beta_{\varepsilon_f} = (\beta_H/\beta_R)$). Then, the scaling testing for the spherical shell can be implemented as the scaling testing for plates in Sect. 3.2.2. The main difference is the power exponent of $\left(\frac{R}{H}\right)$ (or $\left(\frac{\beta_R}{\beta_H}\right)$).

In addition, since the shear and the bending moments are assumed to be zero in this impact model, the number $\Pi_{\sigma_{eq}}^{shell} = \frac{\rho V_z^2}{\sigma_{eq}}\left(\frac{\bar{R}}{\bar{L}_z}\right)$ represents only the effects of the shell membrane force. Therefore, the number $\Pi_{\sigma_{eq}}^{shell}$ reflects the most essential dynamic similarity of shells by the ratio of the inertia force $\left[(\rho\pi\bar{R}^2\bar{L}_z)\left(\frac{V_z^2}{\bar{L}_z}\right)\right]$ to the characteristic of the fully plastic membrane $\left[\sigma_{eq}(\pi\bar{R}\bar{L}_z)\right]$.

In a more general case, the numbers $\Pi_{\sigma_{eq}}$, $\Pi_{\varepsilon_{eq}}$ and $\Pi_{\dot{\varepsilon}_{eq}}$ can be extended to the forms

$$\Pi_{\sigma_{eq}}(n) = \left[\frac{\rho V_z^2}{\sigma_{eq}}\left(\frac{\bar{L}_{xy}}{\bar{L}_z}\right)^n\right], \Pi_{\varepsilon_{eq}}(n) = \left[\varepsilon_{eq}\left(\frac{\bar{L}_{xy}}{\bar{L}_z}\right)^n\right] \text{ and}$$

$$\Pi_{\dot{\varepsilon}_{eq}}(n) = \left[\frac{\dot{\varepsilon}_{eq}\bar{L}_z}{V_z}\left(\frac{\bar{L}_{xy}}{\bar{L}_z}\right)^n\right], \quad \text{(63a-c)}$$

to address the more impact problems by the use of more power exponents for the ratio of characteristic lengths. The intuitive extension is similar to the extension for Zhao's response number in which the original form $R_n = \frac{\rho V_0^2}{\sigma_0}\left(\frac{\bar{L}}{H}\right)^2$ (Zhao, 1998b) is extended to the general form $R_n(n) = \frac{\rho V_0^2}{\sigma_0}\left(\frac{\bar{L}}{H}\right)^n$ (Zhao, 1999) for more impact problems. It can

Preprints (www.preprints.org) | NOT PEER-REVIEWED | Posted: 26 February 2020 doi:10.20944/preprints202002.0394.v1

be learned from the above analysis that the case of $n = 2$ is suitable for the beam and plate subjected to transverse impact; and the case of $n = 1$ is suitable for the spherical shell and cylindrical shells subjected to radial impact. For more power exponent, further verification is needed in future work.

4. Numerical analysis

In this section, a numerical model of circular plate is used for more detailed validation of the ODLV system from the view of point of space deformation and deformation history.

4.1. A clamped circular plate subjected to dynamic pressure pulse

The impact model of a clamped circular plate subjected to two loading cases, as shown in Fig. 5, is now numerically analyzed.

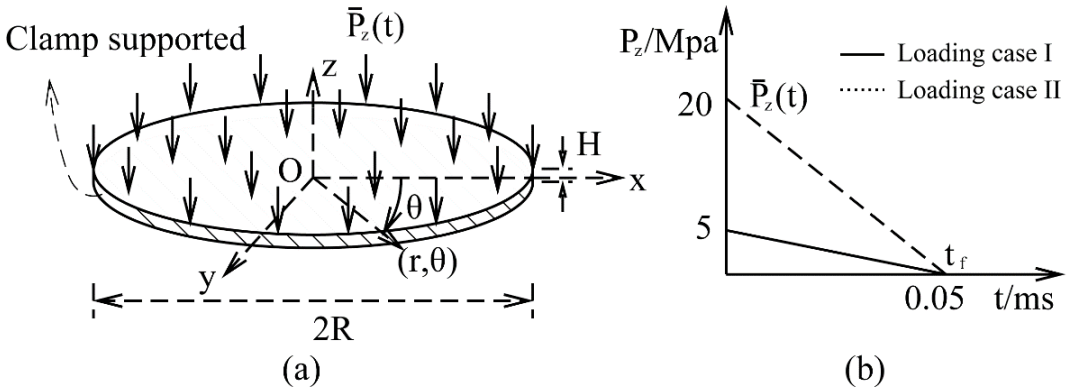

Fig. 5 A clamped circular plate with $R = 125\ mm$ and $H = 2\ mm$ is subjected to pressure pulse loading. (a) clamped circular; (b) pressure pulse.

4.1.1. Numerical modeling

The finite element model of circular plate is modelled in ABAQUS. The CAX4R axisymmetric elements are adopted to discretize structure with 450 elements in radius

Preprints (www.preprints.org) | NOT PEER-REVIEWED | Posted: 26 February 2020 doi:10.20944/preprints202002.0394.v1

and 8 elements in thickness. The clamped external boundary is restrained in cylindrical coordinate system (r, θ, z). The rigid-perfectly plastic material (refering to 1006 Steel (Johnson and Cook, 1983) with $\sigma_d = 350\ MPa$ is adopted to simplify the constitutive equation. The elastic modulus is set 1000 times larger than actual value $E' = 200\ GPa$ to eliminate elastic influence as much as possible. The density of the materials is $7.89 \times 10^3\ kg/m^3$ and Poisson ratio is 0.3. Two loading case, as shown in Fig. 5b, are adopted to study different deformation degrees. According to the impulse theorem $(P_z \pi R^2) t_f/2 = (\rho \pi R^2 H) V_0$, Loading case I and Loading case II are approximately equal to the impulsive velocity $(V_0)_p = 8\ m/s$ and the impulsive velocity $(V_0)_{\mathrm{p}} = 32\ m/s$ on the entire plate, respectively. In addition, for scaled models, four numerical models with $R = 12.5\ mm$ and $H = 0.3,\ 0.4,\ 0.6$ and $0.8\ mm$ are used to verify the validity of the ODLV. The factor $\eta = \beta_H/\beta_R = 1.5, 2, 3\ and\ 4$ is used to represent distortion degree of thickness. The velocity factor β_{V_z} is calculated according to $\beta_{V_z}^{cor} = (\beta_H/\beta_R)\sqrt{\beta_{\sigma_d}/\beta_\rho}$ (Eq. (30)). The amplitude and loading time of dynamic pressure pulse are scaled from the prototype by the factors $\beta_{P_z} = \beta_\rho \left(\beta_{V_z}^{cor}\right)^2$ and $\beta_t = \beta_{L_z}/\beta_{V_z}^{cor}$ (Table 4), respectively. The thickness of four scaled model is discretized with $8\eta = 12, 16, 24, 32$ elements in ABAQUS. Other input conditions of four scaled models are completely identical with the prototype. Finally, scaling factors for input parameters of circular plate are listed in Table 5.

Table 5 Scaling factors for input parameters of circular plate models.

Scaling factor	Prototype	Scaled model $\eta = 1.5$	Scaled model $\eta = 2.0$	Scaled model $\eta = 3.0$	Scaled model $\eta = 4.0$
β_r	1	1/10	1/10	1/10	1/10

Preprints (www.preprints.org) | NOT PEER-REVIEWED | Posted: 26 February 2020 doi:10.20944/preprints202002.0394.v1

β_θ	1	1	1	1	1
β_H	1	0.15	0.2	0.3	0.4
β_ρ	1	1	1	1	1
$\beta_{V_z}^{cor}, \beta_{V_z}$	1	1.5	2	3	4
β_t	1	0.1	0.1	0.1	0.1
β_{P_z}	1	2.25	4	9	16

4.1.2. Results analysis

- **Loading Case I**

(1) Displacement fields

The similarity of displacement fields is evaluated by the displacement components δ_z and δ_r of final time on neutral plane profile, with the results plotted in Fig. 6. Obviously, the displacement components of the prototype and the scaled models are significantly different in the corresponding dimensionless spatial positions ($\Pi_r = \frac{r}{\bar{R}}$), as shown in Fig. 6a and c. While, it can be learned from Table 4 that their values have the scaling relations $\beta_{\delta_z} = \beta_{\bar{L}_z} = 0.15, 0.2, 0.3, 0.4$ and $\beta_{\delta_r} = \beta_{\bar{R}}\left(\beta_{\bar{L}_z}/\beta_{\bar{R}}\right)^2 = 0.25, 0.4, 0.9, 1.6$, respectively. When the numbers $\Pi_{\delta_z} = \frac{\delta_z}{\bar{L}_z}$ and $\Pi_{\delta_r} = \frac{\delta_r}{\bar{R}}\left(\frac{\bar{R}}{\bar{L}_z}\right)^2$ are used to regularize structural response, the dimensionless displacement fields of scaled models behave good consistency with these of prototype on whole deformation profile, as shown in Fig. 6b and d. In addition, the perfect similarity for δ_r, as shown in Fig. 6d, further verifies the reasonableness of the assumptions in Sect. 2.2 for the dimension $dim(\delta_x) = dim(u) = \mathbb{L}_x^{-1}\mathbb{L}_z^2$ in the cartesian coordinate system.

Preprints (www.preprints.org) | NOT PEER-REVIEWED | Posted: 26 February 2020 doi:10.20944/preprints202002.0394.v1

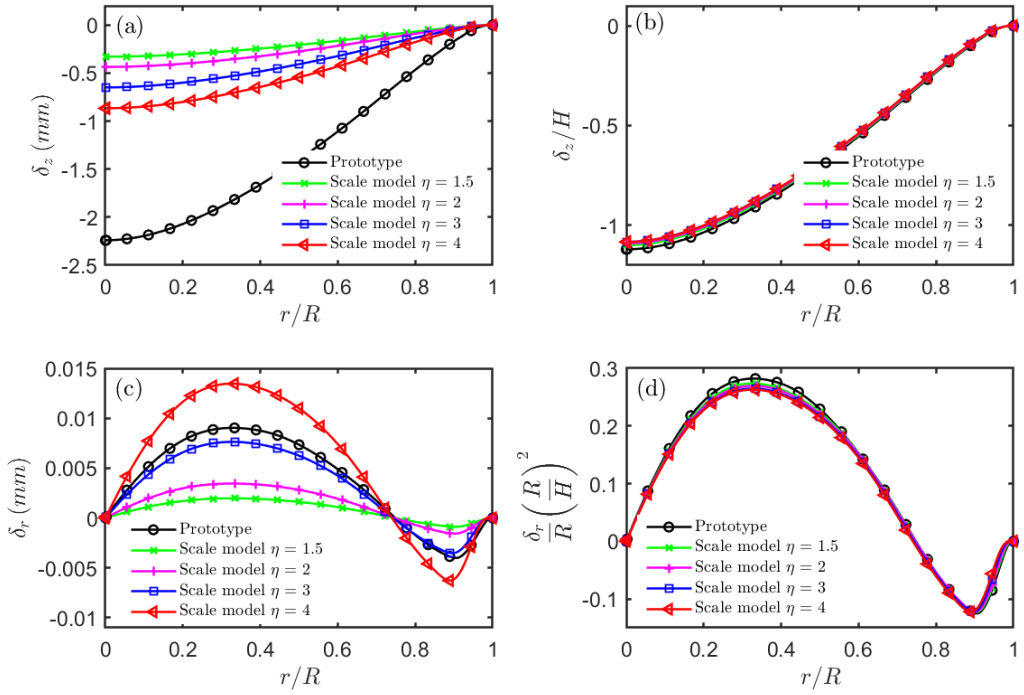

Fig. 6 The neutral plane profile of displacement components for circular plate and scaled models (Loading case I) in final time. (a,b) displacement component δ_z. (c,d) displacement component δ_r.

(2) Stress fields

The similarity of stress fields is evaluated by the stress components σ_r, σ_θ, σ_z and $\tau_{r\theta}$ on neutral plane profile in time $t = (0.3/\beta_t)\ ms$ (or $tV_0/H = 1.2$), with the results plotted in Fig. 7. Obviously, the in-plane stress components σ_r and σ_θ of the scaled models are basically in accordance with these of prototype in the corresponding dimensionless spatial positions, as shown in Fig. 7a and c. While, it can be learned from Table 4 that their values have the scaling relations $\beta_{\sigma_r} = \beta_{\sigma_\theta} = \left(\beta_\rho \beta_{V_z}^2\right)\left(\beta_{\bar{R}}/\beta_{\bar{L}_z}\right)^2 = 1, 1, 1, 1$. However, the transverse stress components σ_z and $\tau_{r\theta}$ are significantly different, as shown in Fig. 7e and g. Their values have the scaling relations $\beta_{\sigma_z} = \left(\beta_\rho \beta_{V_z}^2\right) = 2.25, 4, 9, 16$ and $\beta_{\tau_{r\theta}} = \left(\beta_\rho \beta_{V_z}^2\right)\left(\beta_{\bar{R}}/\beta_{\bar{L}_z}\right) = 1.5, 2, 3, 4$. When the

Preprints (www.preprints.org) | NOT PEER-REVIEWED | Posted: 26 February 2020 doi:10.20944/preprints202002.0394.v1

numbers $\Pi_{\sigma_r} = \frac{\rho V_z^2}{\sigma_r}\left(\frac{\bar{R}}{\bar{L}_z}\right)^2$, $\Pi_{\sigma_\theta} = \frac{\rho V_z^2}{\sigma_\theta}\left(\frac{\bar{R}}{\bar{L}_z}\right)^2$, $\Pi_{\sigma_z} = \frac{\rho V_z^2}{\sigma_z}$ and $\Pi_{\tau_{r\theta}} = \frac{\rho V_z^2}{\tau_{r\theta}}\left(\frac{\bar{R}}{\bar{L}_z}\right)$ are used to regularize structural response, the stress fields of scaled models behave good consistency with these of prototype on whole deformation profile, as expected – Fig. 7b,d,f and h.

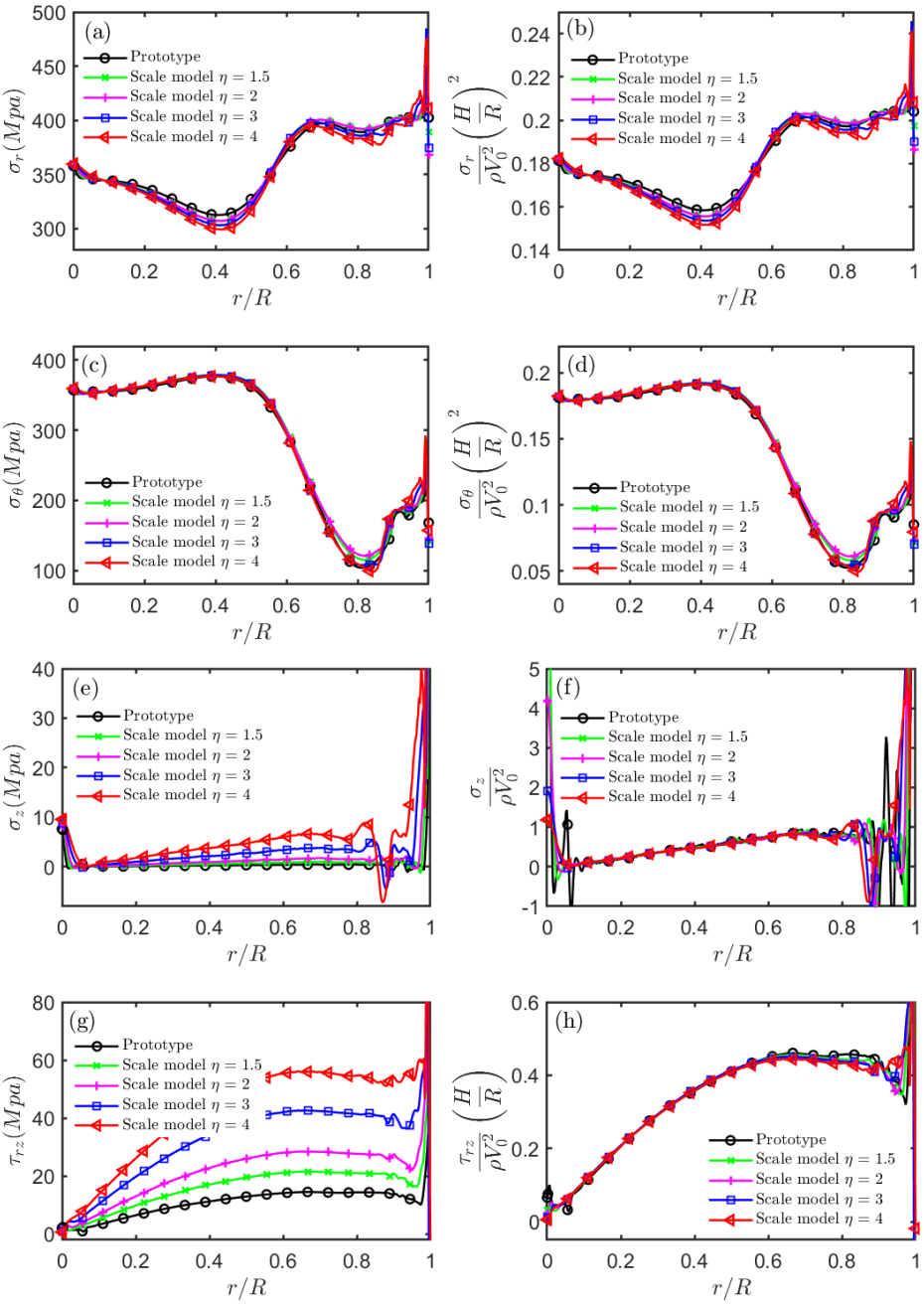

Fig. 7 The neutral plane profile of stress components for circular plate and scaled models in time $t = (0.3/\beta_t)\, ms$ (Loading case I). (a,b) stress component σ_r. (c,d)

Preprints (www.preprints.org) | NOT PEER-REVIEWED | Posted: 26 February 2020 doi:10.20944/preprints202002.0394.v1

stress component σ_θ. (e,f) stress component σ_z. (g,h) stress component $\tau_{r\theta}$.

(3) Strain fields

The similarity of in-plane strain fields is evaluated by the strain components ε_r and ε_θ of final time on neutral plane profile, with the results plotted in Fig. 8. Obviously, the in-plane strain components of the prototype and the scaled models are significantly different in the corresponding dimensionless spatial positions, as shown in Fig. 8a and c. While, it can be learned from Table 4 that their values have scaling relations $\beta_{\varepsilon_r} = \beta_{\varepsilon_\theta} = \left(\beta_{\bar{L}_z}/\beta_{\bar{R}}\right)^2 = 2.25, 4, 9, 16$. When the numbers $\Pi_{\varepsilon_r} = \varepsilon_r \left(\frac{\bar{R}}{\bar{L}_z}\right)^2$ and $\Pi_{\varepsilon_\theta} = \varepsilon_\theta \left(\frac{\bar{R}}{\bar{L}_z}\right)^2$ are used to regularize structural response, the in-plane dimensionless strain fields of scaled models behave good consistency with these of prototype on whole deformation profile, as shown in Fig. 8b and d.

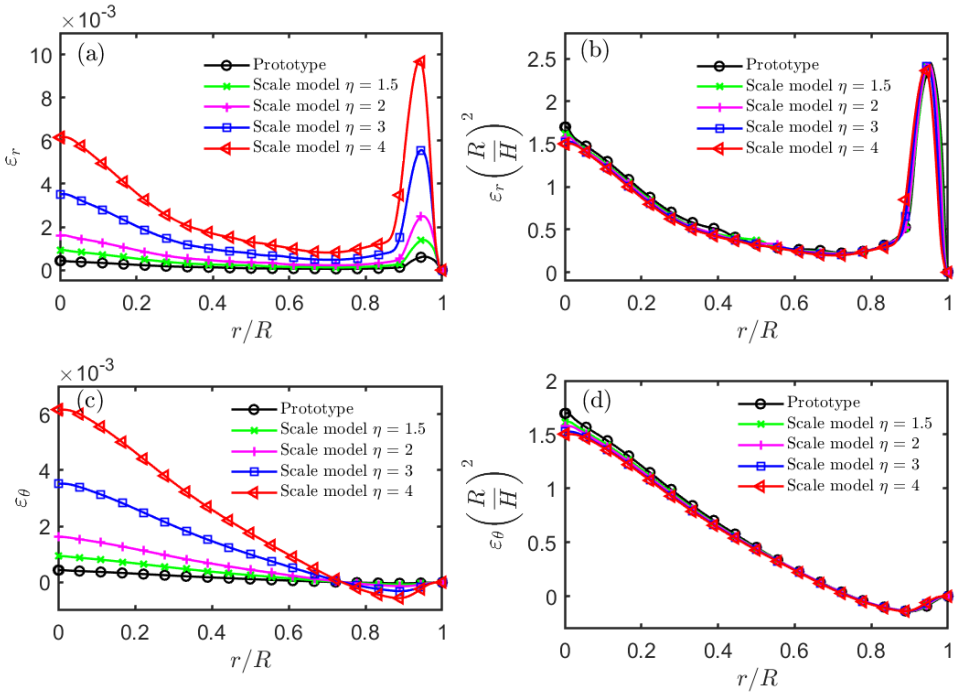

Fig. 8 The neutral plane profile of in-plane strain components for circular plate and scaled models (Loading case I) in final time. (a,b) strain component ε_r. (c,d) strain

Preprints (www.preprints.org) | NOT PEER-REVIEWED | Posted: 26 February 2020 doi:10.20944/preprints202002.0394.v1

component ε_θ.

In order to further verify the reasonableness of oriented dimension analysis for strain components, the decomposed strain components $\varepsilon_r^{u_r} = \frac{\partial u_r}{\partial r}$, $\varepsilon_r^{w} = \frac{1}{2}\left(\frac{\partial w}{\partial r}\right)^2$ from difference calculation of displacements and the synthesized strain component $\left(\varepsilon_r^{u_r} + \varepsilon_r^{w}\right)$ of the neutral plane profile, as shown in Fig. 9, are used to compare the results of Fig. 8a and b. Obviously, the strain components $\varepsilon_r^{u_r}$, ε_r^{w} and $\left(\varepsilon_r^{u_r} + \varepsilon_r^{w}\right)$ for the prototype and the scaled models are significantly different in the corresponding dimensionless spatial positions, as shown in Fig. 9a, c and e. When the numbers $\Pi_{\varepsilon_r^{u_r}} = \varepsilon_r^{u_r}\left(\frac{R}{H}\right)^2$, $\Pi_{\varepsilon_r^{w}} = \varepsilon_r^{w}\left(\frac{R}{H}\right)^2$ and $\Pi_{\left(\varepsilon_r^{u_r}+\varepsilon_r^{w}\right)} = \left(\varepsilon_r^{u_r} + \varepsilon_r^{w}\right)\left(\frac{R}{H}\right)^2$ are used to regularize structural response, the perfect similarity of these dimensionless strain components, as shown in Fig. 9b,d and f, indicates these strain components follow the same similarity law. In addition, when the strain $\varepsilon_r^{u_r}$ and the strain ε_r^{w} are added together, Fig. 9e and f behaves the completely identical dimensionless results with Fig. 8a and b, which verify the correctness for decomposition procedure. Therefore, it can be concluded that the assumption in Sect. 2.2 for the dimension $dim\left(\frac{\partial u}{\partial x}\right) = dim\left(\frac{1}{2}\left(\frac{\partial w}{\partial x}\right)^2\right) = \mathbb{L}_x^{-2}\mathbb{L}_z^2$ of neutral plane strain component $(\varepsilon_x)_{neutral\ plane} = \left(\frac{\partial u}{\partial x}\right) + \frac{1}{2}\left(\frac{\partial w}{\partial x}\right)^2$ are reasonable.

Preprints (www.preprints.org) | NOT PEER-REVIEWED | Posted: 26 February 2020 doi:10.20944/preprints202002.0394.v1

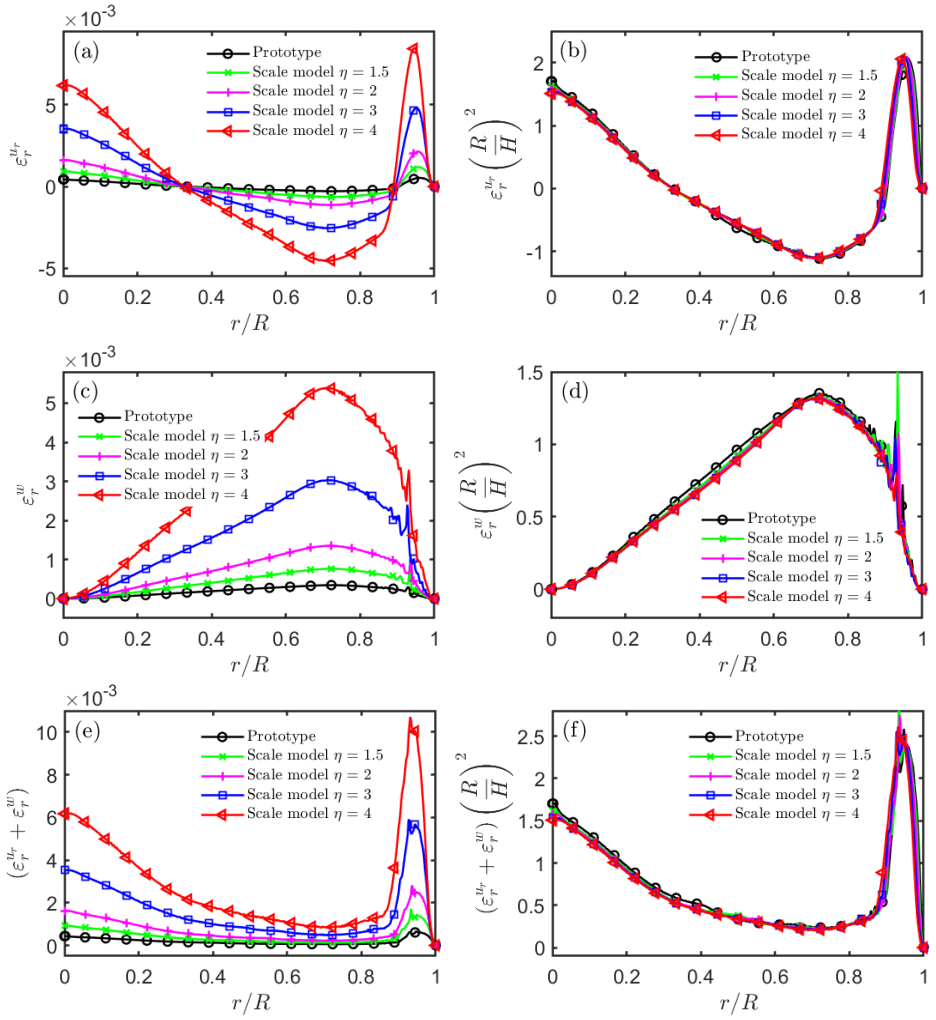

Fig. 9 The neutral plane profile of the decomposed strain components for circular plate and scaled models (Loading case I) in final time. (a,b) strain component $\varepsilon_r^{u_r}$. (c,d) strain component ε_r^{w}. (e,f) strain component $\left(\varepsilon_r^{u_r} + \varepsilon_r^{w}\right)$.

The similarity of transverse strain fields is evaluated by the strain components ε_z and γ_{rz} in final time on neutral plane profile, with the results plotted in Fig. 10. Obviously, the transverse strain components of the prototype and the scaled models are significantly different in the corresponding dimensionless spatial positions, as shown in Fig. 10a and c. While, it can be learned from Table 4 that their values have scaling relations $\beta_{\varepsilon_z}^{mod} = \left(\beta_{\bar{L}_z}/\beta_{\bar{R}}\right)^2 = 2.25, 4, 9, 16$ and $\beta_{\gamma_{rz}}^{mod} = \left(\beta_{\bar{L}_z}/\beta_{\bar{R}}\right)^3 =$

Preprints (www.preprints.org) | NOT PEER-REVIEWED | Posted: 26 February 2020 doi:10.20944/preprints202002.0394.v1

$3.375, 8, 27, 64$. When the numbers $\Pi_{\varepsilon_z}^{mod} = \varepsilon_z \left(\frac{\bar{R}}{\bar{L}_z}\right)^2$ and $\Pi_{\gamma_{rz}}^{mod} = \gamma_{rz} \left(\frac{\bar{R}}{\bar{L}_z}\right)^3$ are used to regularize structural response, the transverse dimensionless strain fields of scaled models behave good consistency with these of prototype on whole deformation profile, as expected – Fig. 10b and d.

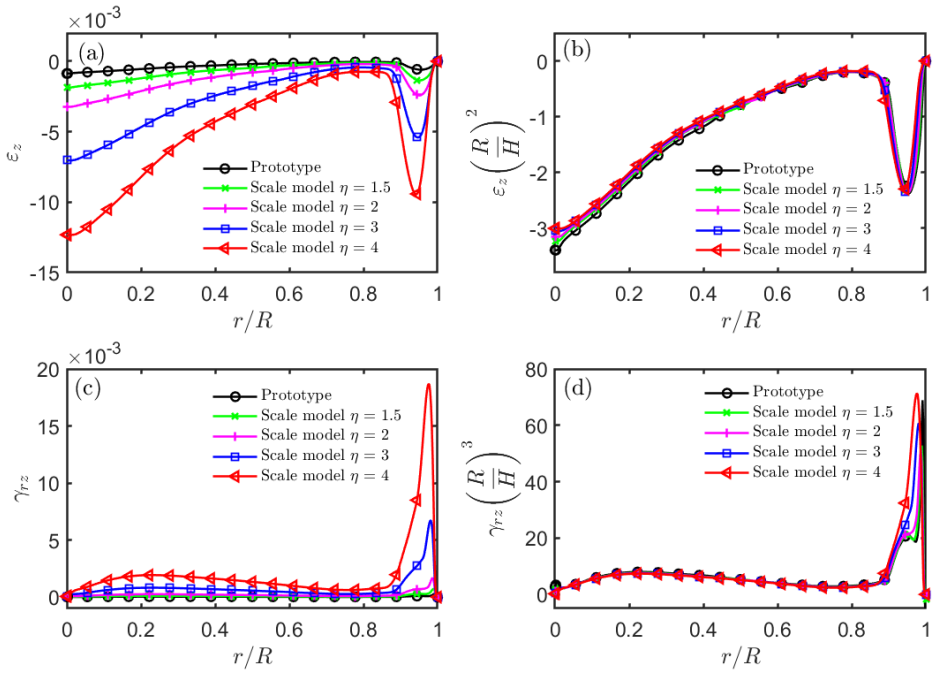

Fig. 10 The neutral plane profile of transverse strain components for circular plate and scaled models (Loading case I) in final time. (a,b) strain component ε_z. (c,d) strain component ε_{rz}.

(4) Equivalent strain fields

The similarity of equivalent strain fields is evaluated by the equivalent strain ε_{eq} of final time on neutral plane profile, with the results plotted in Fig. 11. Obviously, the equivalent strain of the prototype and the scaled models are significantly different in the corresponding dimensionless spatial positions, as shown in Fig. 11a. It can be learned from Table 4 that their values have scaling relation $\beta_{\varepsilon_{eq}} = \left(\beta_{\bar{L}_z}/\beta_{\bar{R}}\right)^2 =$

Preprints (www.preprints.org) | NOT PEER-REVIEWED | Posted: 26 February 2020 doi:10.20944/preprints202002.0394.v1

$2.25, 4, 9, 16$. When the number $\Pi_{\varepsilon_{eq}} = \varepsilon_{eq}\left(\frac{\bar{R}}{\bar{L}_z}\right)^2$ are used to regularize structural response, the dimensionless equivalent strain fields of scaled models behave good consistency with these of prototype on whole deformation profile, as shown in Fig. 11b.

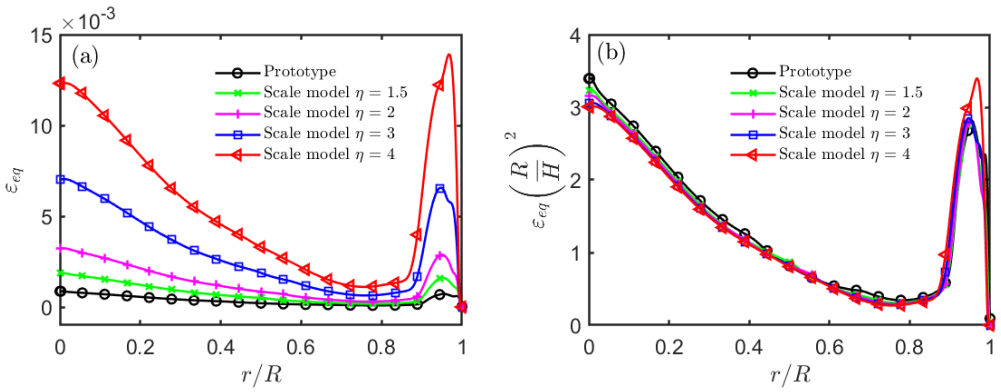

Fig. 11 The neutral plane profile of equivalent strain for circular plate and scaled models (Loading case I) in final time.

(5) Deformation history

The similarity of deformation history is evaluated by four representative physical quantities δ_z, σ_{eq}, ε_{eq} and $\dot{\varepsilon}_{eq}$ at center point, with the dimensionless results plotted in Fig. 12. It is evident from Fig. 12a that the central dimensionless deflections of scaled models have good consistency with these of prototype during deformation history, which results in the maximum dimensionless deflection about $(\delta_z/H)_{max} \approx 1.12$ at final dimensionless time $(tV_0/H)_{final} \approx 1.35$ for prototype and scaled models. For dimensionless equivalent stress $\Pi_{\sigma_{eq}} = \frac{\rho V_z^2}{\sigma_{eq}}\left(\frac{\bar{R}}{\bar{L}_z}\right)^2$, Fig. 12b behaves some significant deviations in the initial small elastic stage, which increases with more large distortion degree η. Nevertheless, the similarity of $\Pi_{\sigma_{eq}}$ is basically in the plastic phase. For dimensionless equivalent strain $\Pi_{\varepsilon_{eq}} = \varepsilon_{eq}\left(\frac{\bar{R}}{\bar{L}_z}\right)^2$ and dimensionless

Preprints (www.preprints.org) | NOT PEER-REVIEWED | Posted: 26 February 2020 doi:10.20944/preprints202002.0394.v1

equivalent strain rate $\Pi_{\dot{\varepsilon}_{eq}} = \frac{\dot{\varepsilon}_{eq}\bar{L}_z}{V_z}\left(\frac{\bar{R}}{\bar{L}_z}\right)^2$, Fig. 12c and d behaves the basically identical results of scaled models and prototype during deformation history.

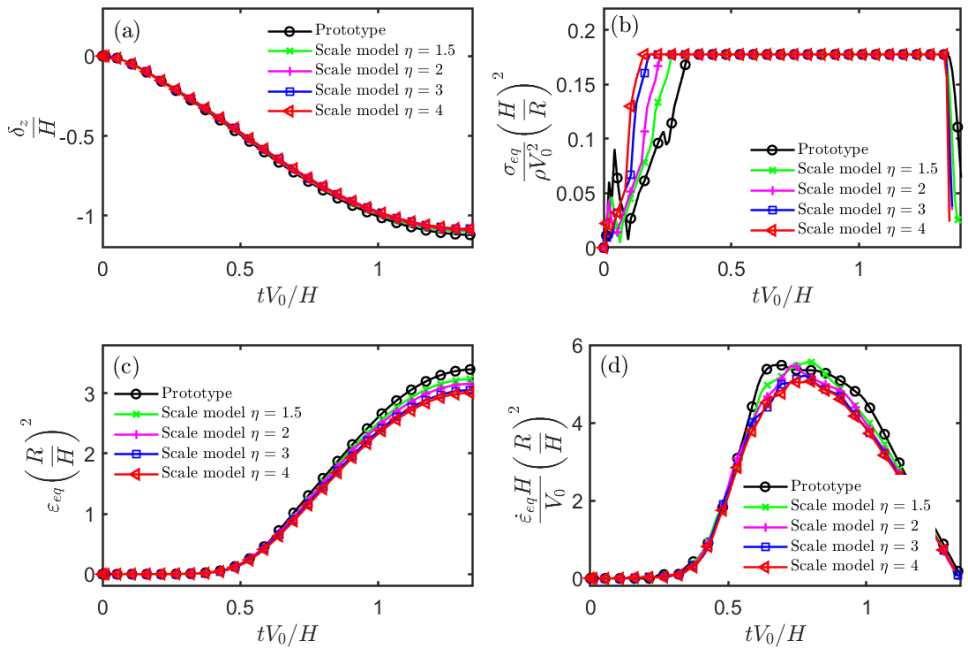

Fig. 12 Main physical quantities of center point during deformation history for circular plate and scaled models (Loading case I). (a) central deflection δ_z. (b) equivalent stress σ_{eq}. (c) equivalent strain ε_{eq}. (d) equivalent strain rate $\dot{\varepsilon}_{eq}$.

- **Loading Case II**

The similarity of the displacement, stress and strain components as well as the equivalent stress, strain and strain rate has been studied in detail under Loading case I, from space deformation and deformation history point of view. For a larger degree of deformation, the Loading case II is used to evaluate the similarity of circular plate. In order to simplify the study, the similarity of displacement components and equivalent strain will be further analyzed in what follows.

(1) Displacement fields

Preprints (www.preprints.org) | NOT PEER-REVIEWED | Posted: 26 February 2020 doi:10.20944/preprints202002.0394.v1

The similarity of displacement fields is evaluated by the displacement components δ_z and δ_r of final time on neutral plane profile, with the results plotted in Fig. 13. It is evident from Fig. 13a, b to Fig. 13c, d that, after using the numbers $\Pi_{\delta_z} = \frac{\delta_z}{\bar{L}_z}$ and $\Pi_{\delta_x} = \frac{\delta_r}{\bar{R}}\left(\frac{\bar{R}}{\bar{L}_z}\right)^2$ to regularize structural response, the dimensionless displacement fields of scaled models become basically in accordance with these of prototype on whole deformation profile. In addition, some small deviations between scaled models and prototype can be observed for the final dimensionless displacements, as shown in Fig. 13b and d, which increase as distortion η increases in the main.

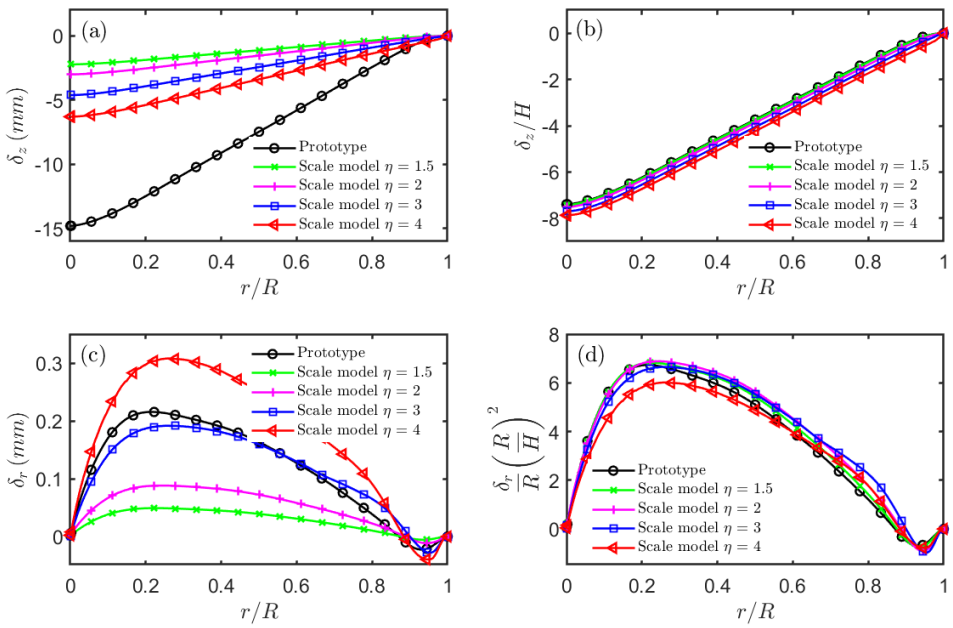

Fig. 13 The neutral plane profile of displacement components for circular plate and scaled models (Loading case II) in final time. (a,b) displacement component δ_z. (c,d) displacement component δ_r.

(2) Equivalent strain fields

The similarity of strain fields is evaluated by the equivalent strain ε_{eq} of final time on neutral plane profile, with the results plotted in Fig. 14. It is evident from Fig.

Preprints (www.preprints.org) | NOT PEER-REVIEWED | Posted: 26 February 2020 doi:10.20944/preprints202002.0394.v1

14a to Fig. 14b that, after using the number $\Pi_{\varepsilon_{eq}} = \varepsilon_{eq}\left(\frac{\bar{R}}{L_z}\right)^2$ to regularize structural response, the dimensionless equivalent strain fields of scaled models become basically in accordance with these of prototype on whole deformation profile. In addition, the relatively obvious deviations can be discovered near the center and root of the circle plates, which increases as distortion η increases in the main. However, for the relatively small distortion $\eta = 1.5$ and 2, these deviations become smaller.

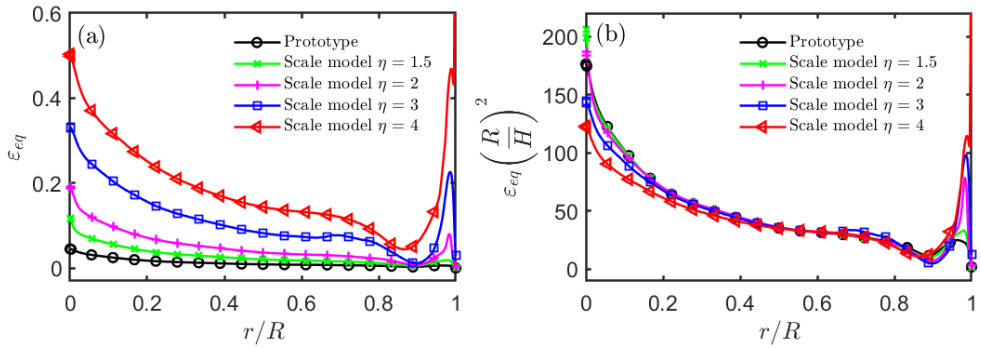

Fig. 14 The neutral plane profile of equivalent strain for circular plate and scaled models (Loading case II) in final time.

(3) Deformation history

The evaluation of displacement and equivalent strain fields indicates that the ODLV similarity laws are still relatively precise for Loading case II from the space deformation point of view. Some deviations for this large deformation case can be attributed to stress σ_z, τ_{rz}, strain ε_{rz} and strain rate $\dot{\varepsilon}_{rz}$ that are not considered in the derivation for the number $\Pi_{\sigma_{eq}}$, the number $\Pi_{\varepsilon_{eq}}$ and the number $\Pi_{\dot{\varepsilon}_{eq}}$ in Sect. 2.3. In order to further evaluate the similarity from the deformation history point of view, two representative physical quantities δ_z and ε_{eq} are plotted in Fig. 15. It is evident from Fig. 15a to Fig. 15b that, after using the number $\Pi_{\delta_z} = \frac{\delta_z}{L_z}$ to regularize

Preprints (www.preprints.org) | NOT PEER-REVIEWED | Posted: 26 February 2020 doi:10.20944/preprints202002.0394.v1

structural response, the dimensionless deflections of scaled models become basically in accordance with these of prototype during deformation history, which results in the maximum dimensionless deflection about $(\delta_z/H)_{max} \approx 8.0$ at final dimensionless time about $(tV_0/H)_{final} = 8.0$. Nonetheless, some small deviations can be found after dimensionless time about $tV_0/H = 4.0$, which increases as distortion η increases. In addition, it is evident from Fig. 15c to Fig. 15d that the significantly different between scaled model and prototype become basically identical when the number $\Pi_{\varepsilon_{eq}} = \varepsilon_{eq}\left(\frac{\bar{R}}{\bar{L}_z}\right)^2$ are used to regularize structural response. Some relatively obvious deviations increase with deformation history after dimensionless time about $tV_0/H = 3.0$, as shown in Fig. 15d. Nonetheless, these deviations can be considered small in comparison to the results of Fig. 15c. However, for relatively small distortion $\eta = 1.5$ and 2, these deviations are decreased significantly.

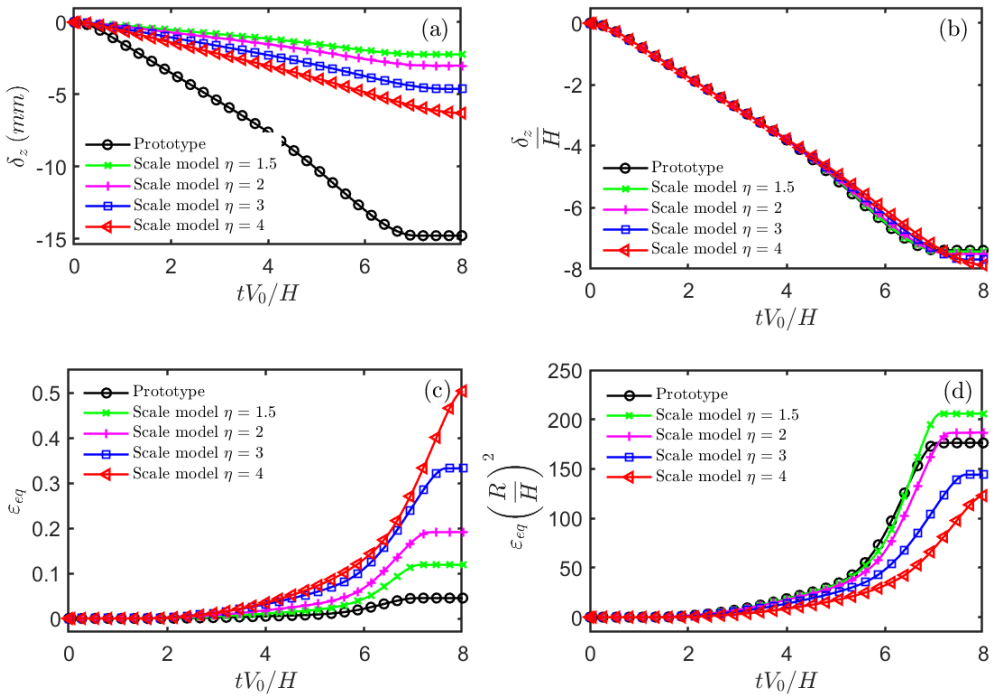

Fig. 15 Main physical quantities of center point during deformation history for

Preprints (www.preprints.org) | NOT PEER-REVIEWED | Posted: 26 February 2020 doi:10.20944/preprints202002.0394.v1

circular plate and scaled models (Loading case II). (a,b) central deflection δ_z. (c,d) equivalent strain ε_{eq}.

In order to analysis the deviations of equivalent strain ε_{eq}, the similarity of transverse shear strain ε_{rz} at a quarter of the neutral plane of the circular plates (i.e., $\Pi_r = \frac{r}{\bar{R}} = \frac{1}{2}$) is evaluated during deformation history, with the results plotted in Fig. 16. It is evident from Fig. 16a to Fig. 16b that, after using the number $\Pi_{\gamma_{rz}}^{mod} = \gamma_{rz}\left(\frac{\bar{R}}{\bar{L}_z}\right)^3$ to regularize structural response, the significantly different between scaled model and prototype become basically identical. After dimensionless time about $tV_0/H = 3.0$, the dimensionless shear strain $\Pi_{\gamma_{rz}}^{mod}$ increases rapidly from very small values, as shown in Fig. 16b. And some degree of deviations increases with the deformation process. However, for relatively small distortion $\eta = 1.5$ and 2, these deviations are decreased significantly. Compared with Loading case I, the dimensionless shear strain of final deformation history $\left(\Pi_{\gamma_{rz}}^{mod}\right)_{final}$ at this spatial position increases significantly —from 5.1 (Fig. 10d) to 951.6 (Fig. 16b). For Loading case I and Loading case II, the dimensionless equivalent strain of final deformation history $\left(\Pi_{\varepsilon_{eq}}\right)_{final}$ at this spatial position are respectively 0.8 (Fig. 11b) and 35.2 (Fig. 15d). Therefore, for final deformation history and this spatial position, the ratio $\left(\Pi_{\gamma_{rz}}^{mod}/\Pi_{\varepsilon_{eq}}\right)_{final}$ is significantly increased from 6.4 of Loading case I to 27.0 of Loading case II, which indicates that the effects of shear strain ε_{rz} for the similarity of equivalent strain ε_{eq} are significantly increased.

Preprints (www.preprints.org) | NOT PEER-REVIEWED | Posted: 26 February 2020 doi:10.20944/preprints202002.0394.v1

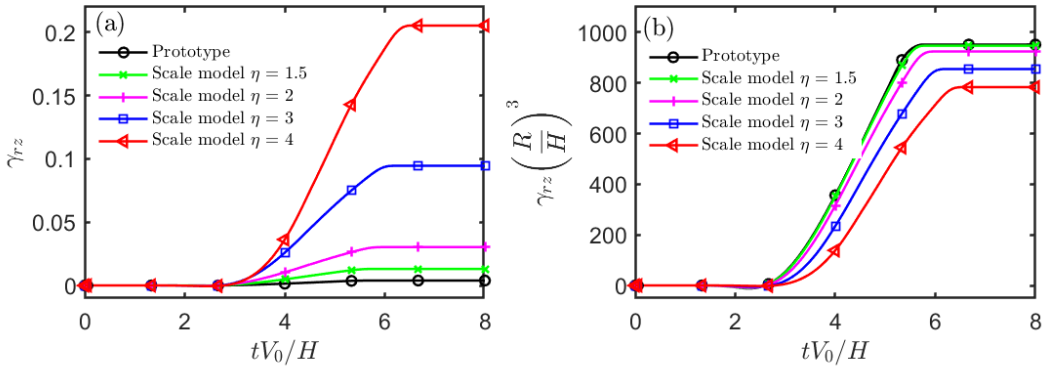

Fig. 16 Transverse shear strain ε_{rz} at a quarter of the neutral plane during deformation history for circular plate and scaled models (Loading case II).

The above analysis for two loading cases shows that, when the ODLV numbers are used to regularize geometric distorted structures, the structural responses for the displacement, stress and strain components and the equivalent stress, strain and strain rate behave the perfect similarity on space deformation and during deformation history. For Loading case I, the ODLV similarity laws are verified to be quite accurate, even for the serious geometrical distortion cases such as $\eta = 3, 4$. For Loading case II, the smaller distortion cases such as $\eta = 1.5, 2$ have a more accurate similarity results while the larger distortion cases such $\eta = 3, 4$ have the certain degree of deviations. In addition, the similarities of stress components σ_r, σ_θ, σ_z and $\tau_{r\theta}$ on neutral plane shows that the proposed similarity laws for the membrane force, the shear force and the normal force are correct. Although stress σ_z, τ_{rz}, strain ε_{rz} and strain rate $\dot{\varepsilon}_{rz}$ that are not considered in the derivations for the numbers $\Pi_{\sigma_{eq}}$, $\Pi_{\varepsilon_{eq}}$ and $\Pi_{\dot{\varepsilon}_{eq}}$, the perfect similarity of all the physical quantities, especially for stress and strain components, indicates that the ODLV system can be used to precise and elaborate analysis for the geometric distorted structures subjected to impact loading.

Preprints (www.preprints.org) | NOT PEER-REVIEWED | Posted: 26 February 2020 doi:10.20944/preprints202002.0394.v1

5. Conclusions

A framework of similarity laws for the geometric distorted structures subjected to impact loading is presented here, which bases on the new prosed oriented-density-length-velocity (ODLV) dimensional analysis. It can be considered as a new progress for similarity laws of structural impact since the influence of three spatial directions and geometric characteristics are expressed effectively. Compared with previous dimensional analysis systems such as MLT, VSG, VSM and DLV, six main aspects are reflected in the new proposed ODLV framework:

(1) A group of oriented dimensions of physical quantity are defined by the oriented analysis for the basic physical definition of physical quantities, the equivalent stress, strain and strain rate and the constitutive relation of the plastic increment theory, which establish the foundation for directional dimensional analysis. Meanwhile, these oriented dimensions are the all-round consideration for all the basic physical quantities from thin-plate impact model that includes six stress components, six strain components, six strain rate components, three displacement components, equivalent stress, equivalent strain, equivalent strain rate, time, external loads and so on.

(2) Five bases, including three oriented characteristic lengths of the geometric space, are used to express the dimensionless number of physical quantities, which instead of three bases of past dimensional analysis system that used only one scalar characteristic length. Therefore, it extends the ability of dimensional analysis for expressing different spatial directions and geometric characteristics.

 doi:10.20944/preprints202002.0394.v1

(3) Three correction methods for the impact velocity, the geometrical thickness and the density are proposed to address different distortion problems such as the geometrical distortion, different materials and gravity, which extends the capabilities of previous correction methods by further considering the effects of structural geometric characteristics.

(4) The most essential dynamic similarity for impact problems is represented by the proposed dimensionless numbers of equivalent stress, stress components and external loadings; for instance, the ratios of inertia moment to the dynamic bending moment (or the fully plastic bending moment), the ratios of inertia force to the structural dynamic force (or fully plastic membrane force or shear force), the ratio of the impact mass to the structural mass. Then, the similarity laws of membrane force, bending moment, shear force and normal force are expressed. In addition, the Zhao's response number is naturally derived by the proposed dimensionless number of equivalent stress; and the differences between the Johnson's damage number D_n and the Zhao's response number R_n are profoundly explained by oriented dimensional analysis of equivalent stress.

(5) The various response equations for impact problems of beam, plate and shell are perfectly expressed by the proposed dimensionless numbers, which improves the defective expression ability of the DLV system for response equations by further considering the direction of physical quantities. In addition, analysis for response equations indicates these dimensionless numbers are important and independent for structural impact.

(6) The precise and elaborate analysis ability for geometric distorted scaled structures is verified in detail by the regularized application of ODLV numbers for the numerical model of impacted circular plates, from the view of point of space deformation and deformation history. And the applicability of these numbers for the serious geometrical distortion and the large deformation are verified, especially for the dimensionless numbers of displacement, stress and strain components.

Since the framework of ODLV is based on the assumptions for thin-plate impact problem, for more complex structures and situations, it needs to be further verified and studied in the future.

Acknowledgements

Writing assistance with Mr. Xiaochuan Liu, Mr. Jijun Liu and Mr. Xulong Xi are gratefully acknowledged. This work is supported by the National Nature Science Foundations of China [grant no. 11972309]; and the Overseas Expertise Introduction Project for Discipline Innovation (the 111 Project) [grant no. BP0719007).

References:

Alves, M., Jones, N., 2002. Impact failure of beams using damage mechanics: part I—analytical model. Int. J. Impact Eng. 27, 837–861. https://doi.org/10.1016/S0734-743X(02)00017-9

Alves, M., Oshiro, R.E., 2006a. Scaling the impact of a mass on a structure. Int. J. Impact Eng. 32, 1158-1173. https://doi.org/10.1016/j.ijimpeng.2004.09.009

Alves, M., Oshiro, R.E., 2006b. Scaling impacted structures when the prototype and the model are made of different materials. Int. J. Solids Struct. 43, 2744-2760. https://doi.org/10.1016/j.ijsolstr.2005.03.003

Booth, E., Collier, D., Miles, J., 1983. Impact scalability of plated steel structures. In: Jones, N., Wierzbicki, T. (Eds.), Structural Crashworthiness, Butterworks, London, pp. 136–174.

Buckingham, E., 1914. On physically similar systems; illustrations of the use of dimensional equations. Phys. Rev. 4, 345-376. https://doi.org/10.1103/PhysRev.4.345

Buckingham, E., 1915. The principle of similitude. Nature 96, 396–397. https://doi.org/10.1038/096396d0

Chien W.Z., 1993. Applied mathematics. Anhui Science and Technology Press, Hefei. (in Chinese)

Drazetic, P., Ravalard, Y., Dacheux, F., Marguet, B., 1994. Applying non-direct similitude technique to the dynamic bending collapse of rectangular section tubes. Int. J. Impact Eng. 15, 797–814. https://doi.org/10.1016/0734-743X(94)90066-T

Fu, S., Gao, X., Chen, X., 2018. The similarity law and its verification of cylindrical lattice shell model under internal explosion. Int. J. Impact Eng. 122, 38–49. https://doi.org/10.1016/j.ijimpeng.2018.08.010

Hu, Y.Q., 2000. Application of response number for dynamic plastic response of plates subjected to impulsive loading. Int. J. Pressure Vessels Piping 77, 711–714. https://doi.org/10.1016/S0308-0161(00)00082-X

Hu, Y.Q., 2009. Dynamic plastic response of beams subjected to impact of concentrated mass. J. Nanjing U. Aeronaut. Astronautics 41, 25-29. https://doi.org/10.16356/j.1005-2615.2009.01.003

Huntley, H.E., 1952. Dimensional analysis. MacDonald & Co. Ltd., London.

Jiang, P., Tian, C.J., Xie, R.Z., Meng, D.S., 2006a. Experimental investigation into scaling laws for conical shells struck by projectiles. Int. J. Impact Eng. 32, 1284–1298. https://doi.org/10.1016/j.ijimpeng.2004.09.015

Jiang, P., Wang, W., Zhang, G.J., 2006b. Size effects in the axial tearing of circular tubes during quasi-static and impact loadings. Int. J. Impact Eng. 32, 2048-2065. https://doi.org/10.1016/j.ijimpeng.2005.07.001

Jiang, Z.R., Zhong, Y.K., Shi K.R., Luo, B., 2016. Gravity-based impact comparability rule of single-layer reticulated shells and its numerical verification. J. South China Univ. Techno. (Nat. Sci. Ed.) 44: 43-48. (in Chinese) https://doi.org/10.3969/j.issn.1000-565X.2016.10.007

Johnson, R., Cook, W.K., 1983. A constitutive model and data for metals subjected to large strains high strain rates and high temperatures. The 7th International Symposium on Ballistics. The Hague, 541-547.

Johnson, W., 1972. Impact strength of materials. Edward Arnold, London.

Jones, N., 1989. Structural impact. Cambridge University Press, Cambridge.

Jones, N., 2012. Impact loading of ductile rectangular plates. Thin Wall. Struct. 50, 68-75. https://doi.org/10.1016/j.tws.2011.09.006

Li, Q.M., Jones, N., 2000. On dimensionless number for dynamic plastic response of structural members. Arch. Appl. Mech. 70, 245–254. https://doi.org/10.1007/s004199900072

Li, Y. L., Zhang, Y.K., Xue, P., 2008. Study of similarity law for bird impact on structure. Chin. J. Aeronaut. 21, 512-517. https://doi.org/10.1016/S1000-9361(08)60168-5

Liu, J.H., Jones, N., 1988. Dynamic response of a rigid plastic clamped beam struck by a mass at any point on the span. Int. J. Solids Struct. 24, 251–270. https://doi.org/10.1016/0020-7683(88)90032-7

Lu, G., Yu, T.X., 2003. Energy absorption of structures and materials. Cambridge Woodhead Publishing, Cambridge.

Mazzariol, L.M., Alves, M., 2019a. Similarity laws of structures under impact load: Geometric and material distortion. Int. J. Mech. Sci. 157-158, 633-647. https://doi.org/10.1016/j.ijmecsci.2019.05.011

Mazzariol, L.M., Alves, M., 2019b. Experimental verification of similarity laws for impacted structures made of different materials. Int. J. Impact Eng. 133, 103364. https://doi.org/10.1016/j.ijimpeng.2019.103364

Mazzariol, L.M., Oshiro, R.E., Alves, M., 2016. A method to represent impacted structures using scaled models made of different materials. Int. J. Impact Eng. 90, 81-94. https://doi.org/10.1016/j.ijimpeng.2015.11.018

Me-Bar, Y., 1997. A method for scaling ballistic penetration phenomena. Int. J. Impact Eng. 19, 821–829. https://doi.org/10.1016/S0734-743X(97)00020-1

Oshiro, R.E., Alves, M., 2004. Scaling impacted structures. Arch. Appl. Mech. 74, 130–145. https://doi.org/10.1007/s00419-004-0343-8

Oshiro, R.E., Alves, M., 2007. Scaling of cylindrical shells under axial impact. Int. J. Impact Eng. 34, 89–103. https://doi.org/10.1016/j.ijimpeng.2006.02.003

Oshiro, R.E., Alves, M., 2009. Scaling of structures subject to impact loads when using a power law constitutive equation. Int. J. Solids Struct. 46, 3412–3421. https://doi.org/10.1016/j.ijsolstr.2009.05.014

Oshiro, R.E., Alves, M., 2012. Predicting the behaviour of structures under impact loads using geometrically distorted scaled models. J. Mech. Phys. Solids 60, 1330-1349. https://doi.org/10.1016/j.jmps.2012.03.005

Parkes, E.W., 1955. The permanent deformation of a cantilever struck transversely at its tip. P. Roy. Soc. Lond. A Mat. 228, 462-476. https://doi.org/10.1098/rspa.1955.0062

Reddy., J.N., 2007. Theory and analysis of elastic plates and shells (Second Edition). CRC Press ; Taylor & Francis Group.

Sadeghi, H., Davey, K., Darvizeh, R., Darvizeh, A., 2019a. A scaled framework for strain rate sensitive structures subjected to high rate impact loading. Int. J. Impact Eng. 125, 229-245. https://doi.org/10.1016/j.ijimpeng.2018.11.008

Sadeghi, H., Alitavoli, M., Darvizeh, A., Rajabiehfard, R., 2019b. Dynamic plastic behaviour of strain rate sensitive tubes under axial impact. Thin Wall. Struct., 143, 106220. https://doi.org/10.1016/j.tws.2019.106220

Shi, X.H., Gao, Y.G., 2001. Generalization of response number for dynamic plastic response of shells subjected to impulsive loading. Int. J. Pressure Vessels Piping 78, 453–459. https://doi.org/10.1016/S0308-0161(01)00050-3

Wang, S., Xu, F., Dai, Z., 2019. Suggestion of the DLV dimensionless number system to represent the scaled behavior of structures under impact loads. Arch. Appl. Mech. https://doi.org/10.1007/s00419-019-01635-9

Wei, D., Hu, C., 2019. Scaling of an impacted reticulated dome using partial similitude method. Lat. Am. J. Solids Struct. 16, e158. https://doi.org/10.1590/1679-78255342

Yu, T. X., Xue, P., 2010. Engineering plastic mechanics. China Higher Education Press, Beijing (in Chinese).

Yu, T. X., Qiu, X. M., 2018. Introduction to Impact Dynamics. Tsinghua University Press, Beijing.

Zhao, Y.P., 1998a. Prediction of structural dynamic plastic shear failure by Johnson's damage number. Forsch. Ingenieurwes. 63, 349-352. https://doi.org/10.1007/PL00010753

Zhao, Y.P., 1998b. Suggestion of a new dimensionless number for dynamic plastic response of beams and plates. Arch. Appl. Mech. 68, 524–538. https://doi.org/10.1007/s004190050184

Zhao, Y.P., 1999. Similarity consideration of structural bifurcation buckling. Forsch. Ingenieurwes. 65, 107-112. https://doi.org/10.1007/PL00010868